

UC San Diego

Research Theses and Dissertations

Title

Development of a Cellular Model of Rheumatoid Arthritis: The Study of Marine Natural Products in the Disease Milieu

Permalink

<https://escholarship.org/uc/item/09m422fk>

Author

McGough, Kevin A.

Publication Date

2000-04-01

Peer reviewed

INFORMATION TO USERS

This manuscript has been reproduced from the microfilm master. UMI films the text directly from the original or copy submitted. Thus, some thesis and dissertation copies are in typewriter face, while others may be from any type of computer printer.

The quality of this reproduction is dependent upon the quality of the copy submitted. Broken or indistinct print, colored or poor quality illustrations and photographs, print bleedthrough, substandard margins, and improper alignment can adversely affect reproduction.

In the unlikely event that the author did not send UMI a complete manuscript and there are missing pages, these will be noted. Also, if unauthorized copyright material had to be removed, a note will indicate the deletion.

Oversize materials (e.g., maps, drawings, charts) are reproduced by sectioning the original, beginning at the upper left-hand corner and continuing from left to right in equal sections with small overlaps.

Photographs included in the original manuscript have been reproduced xerographically in this copy. Higher quality 6" x 9" black and white photographic prints are available for any photographs or illustrations appearing in this copy for an additional charge. Contact UMI directly to order.

Bell & Howell Information and Learning
300 North Zeeb Road, Ann Arbor, MI 48106-1346 USA
800-521-0600

UMI[®]

**University of California
Santa Barbara**

**Development of a Cellular Model of Rheumatoid
Arthritis: The Study of Marine Natural Products in
the Disease Milieu.**

A Dissertation submitted in partial satisfaction of the
requirements for the degree of

Doctor of Philosophy

In

Biology

By

Kevin A. McGough

Committee members:

Professor Robert S. Jacobs, Chairman

Professor Armand Kuris

James D. Winkler Ph.D.

April 2000

UMI Number: 3001467

UMI[®]

UMI Microform 3001467

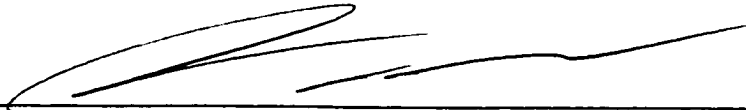
Copyright 2001 by Bell & Howell Information and Learning Company.

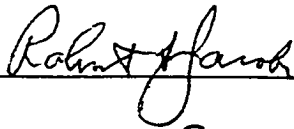
All rights reserved. This microform edition is protected against
unauthorized copying under Title 17, United States Code.

Bell & Howell Information and Learning Company
300 North Zeeb Road
P.O. Box 1346
Ann Arbor, MI 48106-1346

The Dissertation of Kevin Æ McGough is approved by:







Committee Chairperson

April 2000

Acknowledgements

I want to thank my committee and chairman for their patience, understanding and positive input throughout my graduate career. I would like to acknowledge the California Sea Grant College for funding my research under program grants NA-36RG0537 and NA-66RG0477 and SmithKline Beecham Pharmaceuticals for matching funds in California Sea Grant Industrial Fellowship IF-1. I would also like to mention Dr. William Gerwick (Oregon State University, College of Pharmacy), without whose contribution of natural products, this research would have been impossible.

Dedication

Edward Paul McGough

1931-1999

Vita

1969 Born Flint, MI
1987 Central Catholic High School Pittsburgh, PA
1991 B,S Fairleigh Dickinson University Teaneck, NJ
1992-1997 Teaching Assistant, UCSB
1995 MA, UCSB
1995-1996 Intern, SmithKline Beecham, King of Prussia, PA
1998 Teaching Associate, UCSB
1998-2000 Instructor, State University of New York, Stony Brook

Publications

Amy K. Roshak, Jeffrey R. Jackson, Kevin McGough, Marie Chabot-Fletcher, Eugene Mochan, and Lisa A. Marshall. Manipulation of Distinct NF κ B Proteins Alters Interleukin-1-induced Human Rheumatoid Synovial Fibroblast Prostaglandin E₂ Formation. *J. Biol. Chem.* 1996 Dec 06; 271 (49): 31496-31501.

McGough KA; Jackson JR; Minton JA; Marshall LA; Jacobs RS; Winkler JD. Inflammatory PGE₂ production is maintained during hypoxia in rheumatoid synovial fibroblasts. *Inflammation Research* 46 Suppl. 1996. (2):S147-8.

Lik Tong Tan, Thomas Williamson, Shawn Watts, William Gerwick, Kevin McGough, Robert Jacobs. *Cis, cis* and *Trans, trans*-Ceratospongamide, New Bioactive hepatapeptides from the Indonesian red Alga *Ceratdictyon spongiosum*. *J. Org. Chem.* In submission.

Workshops and
Posters

Kevin A. McGough, Namthip Sitachitta†, Tan Lik Tong†, Angie Nguyen, William H. Gerwick† and Robert S. Jacobs. Bioassay Guided Purification: Marine Natural Products Purified Through a New Secreted Phospholipase A₂ Cellular Screening Model. Workshop: Marine Natural Products, Gordon Research Conferences.

Amy K. Roshak, Jeffrey R. Jackson, Kevin McGough, Marie Chabot-Fletcher, Eugene Mochan, and Lisa A. Marshall. NFκB Participates in the Regulation of IL-1β-Induced Human Rheumatoid Synovial Fibroblast Prostaglandin E₂ Formation. Workshop: Eighth International Conference of the Inflammation Research Association, October 1996, Hershey, PA.

Kevin McGough, J.R. Jackson, J.A. Minton, L.A. Marshall, R.S. Jacobs and J.D. Winkler. Inflammatory PGE₂ Production is Maintained During Hypoxia in Rheumatoid Synovial Fibroblasts. Poster Session: Eighth International Conference of the Inflammation Research Association, October 1996, Hershey, PA.

Kevin McGough and R.S. Jacobs. The dynamics of Phospholipase A₂ in the marine sponge *Lucretia* (*Leuconia*) *losangelensis*. Workshop: First Annual Meeting of the Florida Sponge Society "Sponges: A Multidisciplinary Approach". September 1992, Harbor Branch Oceanographic Institution, Fort Pierce, FL.

Abstract

Development of a Cellular Model of Rheumatoid Arthritis: The Study of Marine Natural Products in the Disease Milieu.

Kevin A McGough

This dissertation is focused upon the study and pharmacological treatment of an inflammatory hallmark of rheumatoid arthritis. It involved the following phases: 1) The development and study of cellular models of rheumatoid arthritis. 2) The bioassay guided fractionation of 124 marine extracts. 3) The characterization of two purified compounds discovered through the bioassay model.

- 1 The initial phase of the work studied rheumatoid arthritis synoviocytes. These cells have an altered phenotype in the disease milieu. The production of 14kDa secreted Phospholipase A₂ (sPLA₂) by these cells was studied, and a secondary cellular model was developed through this study. The bioassay derived from this phase of study employed the human hepatoma cell line HepG2. Interleukin-1 β was used to recreate the disease characteristic of the rheumatoid fibroblasts in this second cell type.

Through several stages of guided fractionation, a dozen primary candidate extracts were ultimately reduced to two. Subsequently, these two active extracts were purified to homogeneity.

- 3 The first of these compounds was *trans-trans* ceratospongamide. This cyclic peptide was first co-purified with a conformer, *cis-cis* ceratospongamide. The *trans-trans* form has an ED₅₀ of 32 nM in the HepG2 model. The *cis-cis* form is inactive. Reporter and electrophoretic mobility shift assays indicated that the AP-1 pathway of cytokine signaling was a potential site of action for the active molecule. The second molecule, kalkitoxin, was purified after six stages of fractionation. In unpublished work, this molecule had previously been found ichthyotoxic and invertibraticidal. In the HepG2 model, this molecule has an ED₅₀ of 7 nM. Subsequent studies showed that this molecule was active in an assay sensitive to microtubule poisons. The IL-1 β signaling pathway leading to sPLA₂ release is also very susceptible to microtubule poisons, and thus, it appears that kalkitoxin may be acting at this level in the bioassay.

Table of Contents

<i>Dedication</i>	<i>iii</i>
<i>Vita.....</i>	<i>v</i>
<i>Abstract.....</i>	<i>vii</i>
<i>Table of Contents</i>	<i>ix</i>
<i>Table of Tables</i>	<i>xviii</i>
<i>1 Introduction.....</i>	<i>1</i>
<i>1.1 Background.....</i>	<i>2</i>
<i>1.2 The Diseased Synovium</i>	<i>6</i>
1.2.1 Clinical Diagnosis	6
1.2.2 Cellular Morphology.....	8
1.2.3 Altered Gene Expression	9
1.2.4 Chemotactic factors.....	10
1.2.5 Adhesion Molecules	11
1.2.6 Hydrolytic and Oxidizing Enzymes	12
<i>1.3 Pharmacological Modulation of Rheumatoid Disease</i>	<i>16</i>
1.3.1 Steroidal Intervention.....	16

1.3.2	PLA ₂ Inhibitors.....	18
1.3.3	Transcriptional regulation.....	20
1.4	Cellular Models of Inflammatory Disease.....	23
1.4.1	Synoviocytes.....	23
1.4.2	Normal Fibroblasts	23
1.4.3	HepG2 Cells	26
2	Methods.....	27
2.1	Cell Culture.	27
2.1.1	Human Rheumatoid Synovial Fibroblasts	27
2.1.2	HepG2.....	28
2.2	Hypoxia Studies in Human Rheumatoid Synovial Fibroblasts.....	29
2.3	Type II PLA₂ ELISA.....	29
2.4	PGE₂ ELISA.....	32
2.5	Preparation of Plasmids for CAT Reporter Assay.	33
2.6	Transfection of HepG2 cells with sPLA₂ promoter-CAT Constructs.	36
2.7	Chloramphenical Acetyl Transferase ELISA.....	38

2.8	Electrophoretic Mobility Shift Assay (EMSA)	39
2.9	Bioassay-Guided Marine Natural Product Studies	44
2.10	LDH Release Assay	46
2.11	MTT Mitochondrial Viability Assay	47
2.12	Sea Urchin Embryo Assay	48
2.13	Purified Microtubule Complex Interference	49
3	<i>Results</i>	51
3.1	Cellular Models	51
3.1.1	Rheumatoid Fibroblasts.....	51
3.1.2	Normal Human Lung Fibroblasts.....	55
3.1.3	HepG2 Cells	57
3.2	Bioassay-Guided fractionation	62
3.3	Pharmacological Studies	84
3.3.1	Kalkitoxin	84
3.3.2	Ceratospongamides.....	89
4	<i>Conclusions</i>	105
4.1	Model Development	105
4.2	Target Selection	105

4.3	Model Profiling	107
4.4	Pharmacological Studies of <i>Ceratodictyon spongiosum</i> extracts.	108
4.4.1	Sea Urchin Assay	109
4.4.2	CAT Reporter Assay.....	110
4.4.3	Electrophoretic Mobility Shift Assay	111
4.5	Pharmacological Studies of <u><i>Lyngbya majuscula</i></u>.....	112
4.5.1	Microtubule Studies.....	113
4.6	Future Work	114
4.6.1	Northern Blot analysis.	115
4.6.2	Electrophoretic Mobility Shift Assay with increased replicates and Supershift Studies.	117
4.6.3	Purified Microtubule Assays	117
4.6.4	Additional <i>In vitro</i> studies.	118
5	<i>Bibliography</i>.....	119

Table of Figures

<i>Figure 1. The Rheumatoid Joint: Comparison of healthy (Left) and diseased (Right) synovial tissue.</i>	<i>7</i>
<i>Figure 2. RSF-Derived PGE₂ after 24 hours of incubation in a hypoxic chamber ± IL-1β (10 ng/ml). N=3.</i>	<i>52</i>
<i>Figure 3. Dose Response(PGE₂ production) of IL-1β on cultured Rheumatoid Synovial Fibroblasts (RSF) over 24 hours. Error bars represent one standard deviation, N=3.</i>	<i>54</i>
<i>Figure 4. The effect of IL-1β on the secretion of PLA₂ from RSF over 24 hours. N=3.....</i>	<i>55</i>
<i>Figure 5. A study of the effect of hypoxia (H), normoxia (N) and IL-1β (1 ng/ml) on RSF (S) and NHLF (L) -derived PGE₂. Error bars represent one standard deviation, N=12.....</i>	<i>56</i>
<i>Figure 6. The effects of pro-inflammatory cytokines on the expression of sPLA₂ in HepG2 cells over 48 hours. Error bars represent one standard deviation, N=8.....</i>	<i>58</i>
<i>Figure 7. Effect of human-IL-1β (400 pg/ml) on HepG2 cells over time. Error expressed as one standard deviation, N=6.</i>	<i>59</i>
<i>Figure 8. The effect of increasing concentration of IL-1β on HepG2 cells over a 24-hour period. Error bars represent one standard deviation, N=12.</i>	<i>60</i>

Figure 9. Comparison of the biological activity from the first round of fractionation in the HepG2 model of inflammation. Error expressed as one standard deviation, Numbers represent % inhibition, parentheses > 100% stimulation, N=6..... 67

Figure 10. Comparison of the biological activity from the first round of fractionation in the HepG2 model of inflammation. Error expressed as one standard deviation, Numbers represent % inhibition, parentheses > 100% stimulation, N=6..... 68

Figure 11. Comparison of the biological activity from the first round of fractionation in the HepG2 model of inflammation. Error expressed as one standard deviation, Numbers represent % inhibition, parentheses > 100% stimulation, N=6..... 69

Figure 12. Comparison of the biological activity from the first round of fractionation in the HepG2 model of inflammation. Error expressed as one standard deviation, Numbers represent % inhibition, parentheses > 100% stimulation, N=6..... 70

Figure 13. Comparison of the biological activity from the first round of fractionation in the HepG2 model of inflammation. Error expressed as standard deviation, Numbers represent % inhibition, parentheses > 100% stimulation, N=6..... 71

Figure 14. Comparison of the biological activity from the first round of fractionation in the HepG2 model of inflammation. Error expressed as standard

<i>deviation, Numbers represent % inhibition, parentheses > 100% stimulation, N=6.....</i>	<i>72</i>
<i>Figure 15. Comparison of the biological activity from the first round of fractionation in the HepG2 model of inflammation. Error expressed as standard deviation, Numbers represent % inhibition, parentheses > 100% stimulation, N=6.....</i>	
<i>73</i>	
<i>Figure 16. Comparison of the biological activity from the first round of fractionation in the HepG2 model of inflammation. Error expressed as standard deviation, Numbers represent % inhibition, parentheses > 100% stimulation, N=6.....</i>	
<i>74</i>	
<i>Figure 17. Comparison of the biological activity from the first round of fractionation in the HepG2 model of inflammation. Error expressed as standard deviation, Numbers represent % inhibition, parentheses > 100% stimulation, N=6.....</i>	
<i>75</i>	
<i>Figure 18. Purification tree for WG-933. Percent inhibition of sPLA₂ in the HepG2 model of inflammation expressed for each extract. Red bubbles represent extracts taken to the next tier of purification, N=6.....</i>	
<i>78</i>	
<i>Figure 19. Malyngamide H.....</i>	
<i>78</i>	
<i>Figure 20. Several Malyngamides were tested at 1µg/ml in the HepG2 model of inflammation. (A: Malyngamide C, B: Malyngamide C-acetate, C: Malyngamide F-acetate, D: Malyngamide H, E: Malyngamide I, F: Malyngamide J, G:</i>	

Malyngamide L, H: Malyngolide) Error expressed as one standard deviation,
Numbers represent %, inhibition, parentheses > 100% stimulation, N=6... 79

Figure 21. Comparison of the biological activity of methylation products
formed in the GC/MS analysis of WG-933D2B,C in the HepG2 model of
inflammation. (A: WG-933-D2B 10µg/ml, B: WG-933-D2B 1µg/ml, C: WG-
933-D2B-O-Me 10µg/ml, D: WG- 81

Figure 22. Kalkitoxin 81

Figure 23. Curacin A..... 82

Figure 24. The effect of the Microtubule Destabilizing Compounds (MTD)
Curacin A and Vinblastine in HepG2 sPLA₂. Error bars represent one standard
deviation, N=6. 83

Figure 25. The effect of the active fraction from the HepG2 model of
inflammation on the rate of fertilized sea urchin embryos reaching the 2-celled
(A) and 4-celled (B) stages of division, N≥200. 87

Figure 26. Dose/response of HepG2 cells to WG-933 D2C5. The bars represent
the number of hours required to pass greater than 90% of viable embryos
through the first division (N≥200). The curve and boxes with standard error
expressed as standard deviation, represent the dose/response of HepG2 cells
to WG-933 D2C5, N=6. 88

Figure 27. Ceratospongamides A and B. 91

Figure 28. Log-dose/response relationship for trans-trans ceratospongamide in
the HepG2 model. Error bars represent one standard deviation, N=6..... 92

Figure 29. Bars represent the time required (hours) for at least 90% of viable embryos to reach the first () or second () cell division. Vehicle is DMSO 0.1%. Less than 0.5% cytotoxicity for all treatments, 97% fertilization efficiency, Strongylocentrotus purpuratus, N>300. 95

Figure 30. The left Y-Axis and bars represent the number of hours required to pass greater than 90% of viable embryos through the first division (N>200). The right Y-Axis and line represent the dose/response of HepG2 cells to trans-trans Ceratospongamide. Error expressed as standard deviation, (N=6). 97

Figure 31. The proximal portion of the sPLA2 promoter. The IL-6 regulated elements A-D are color coded pink, green, light and dark blue respectively. Interleukin-sensitive elements are marked in the sequence by bars..... 100

Figure 32. Electrophoretic Mobility Shift Assay for AP-1 consensus sequence binding. Control (A), IL-1 β stimulated (B) and trans-trans Ceratospongamide pretreated, IL-1 β stimulated (C) HepG2 nuclear extracts were tested. Lane A.1 lacks nuclear extracts as 103

Table of Tables

<i>Table 1. Inflammatory materials induced in rheumatoid cells by the disease state.</i>	<i>9</i>
<i>Table 2. Electrophoretic Mobility Shift Assay Labeling Reaction.</i>	<i>41</i>
<i>Table 3. Labeling reactions for nuclear extracts.</i>	<i>42</i>
<i>Table 4. . Slab gels (16 cm x 10 cm x 0.75 mm) were prepared by combining the above reagents.</i>	<i>43</i>
<i>Table 5. The table above represents the effects of drugs having inhibitory effects at various points of the inflammatory cascade as observed in HepG2 cells, N=6.</i>	<i>61</i>
<i>Table 6. Preliminary bioassay of various marine extracts in the HepG2 model of inflammation. Columns represent the chemist's designation, Phylum, Genus and species (if available), and percent inhibition of sPLA₂ secretion in the model (N≥6).</i>	<i>66</i>
<i>Table 7. The cyclic peptides above were tested under identical conditions to trans-trans ceratospongamide. Negative numbers</i>	<i>93</i>
<i>Table 8. Consensus oligonucleotides used in the AP-1 Electrophoretic Mobility Shift assay.</i>	<i>104</i>

1 Introduction

The objective of this dissertation is to use a facet of rheumatoid arthritis as a model of an inflammatory disease state to investigate marine natural products in the expression of an inflammatory synthetic pathway. The hallmark of rheumatoid arthritis is the hyperplasia of joint synovium causing destruction of cartilage, and bone by this invasive inflammatory tissue, called the pannus. The altered pattern of gene expression that produces the altered phenotype of pannus fibroblasts and endothelial cells is controlled by an aberrant activation of various transcription factors and results in accumulation of secreted phospholipase A₂. This project establishes cellular models of inflammatory gene expression, characterizes these models, and attempts to explore the role which marine natural products play in attenuating the expression and release of the acute-phase gene product, secreted phospholipase A₂.

Models were established specifically to investigate the effects of marine natural products on the expression of the inflammatory

enzyme sPLA₂ and to guide the isolation of novel molecules. These marine natural products will further the understanding of inflammatory diseases through characterization of the molecular events in the progression of rheumatoid arthritis.

1.1 Background

Rheumatoid arthritis (RA) is the most common chronic inflammatory disease, causing debilitating joint destruction in both children and adults. The incidence of the disease approaches 1% of the world population. Rheumatoid arthritis is inexorably progressive because current pharmacological intervention is palliative, not curative. Most therapeutic regimes include classical, broad-spectrum analgesics and in some instances mild immunosuppressive agents [Caldwell 1995]. As prophylactic measures, NSAIDs and steroidal anti-inflammatory compounds have no positive effects; the use of cyclooxygenase inhibitors may actually be responsible for accelerated progression of the disease [Case 1990]. Current therapy for all inflammatory disease states is unsatisfactory. Novel therapeutic approaches developed from

models of cellular inflammation may have an enormous impact globally on both rheumatoid arthritis and other diseases that involve an aberrant inflammatory response.

The role of the inflammatory response in the pathogenesis of disease is currently an area of much interest in the biomedical sciences. Molecular characterization is clarifying classic chronic inflammatory diseases, such as rheumatoid arthritis, systemic lupus erythematosus, periodontal degradation, sepsis and tumor growth. Inflammation associated with rheumatoid arthritis can be divided into 4 stages in humans [Pruzanski 1991]. 1) Injurious agents enter the body in the form of pathogenic organisms, deleterious compounds, physical trauma or altered (transformed) cells. These agents act upon specific target cells and activate them. 2) At this stage, the immune cells, synoviocytes, polymorphonuclear leukocytes and mast cells up-regulate the synthesis or activation of Phospholipases A₂ (PLA₂) and other pro-inflammatory enzymes resulting in their accumulation in the joint synovium. 3) Following the proliferative effect of the initial

inflammatory signal, the cascade of activation results in a more generalized activation of the cytokines Interleukin-1 (IL-1) and Tumor Necrosis Factor (TNF), these paracrine factors short-circuit the initial step of inflammation. 4) The final stage in the inflammatory response is the activation and release of arachidonic acid and its downstream metabolites, the leukotrienes, lipoxins, prostaglandins, prostacyclins and thromboxanes. These molecules, along with lyso-phosphatidylcholine (1-acyl, 2-OH phosphatidylcholine, cause chemotaxis, mitogenesis, adhesion, vascular permeability, calcium release, increase of collagenase and elastase release and a host of related physiological responses associated with inflammation. Therefore the importance of detecting the initial inflammatory signal inciting disease, or at least, blocking the initial response to that signal, has become a major goal.

Attempts to find a pathogen responsible for inducing the inflammatory disease rheumatoid arthritis have been unsuccessful. As a consequence of this, a great deal of

inflammation research has been aimed at the second step of the inflammatory process where IL-1, PAF, and TNF all show activity in up-regulating inflammatory pathways [Glaser 1993]. These cytokines act via various intracellular messengers. This second messenger mediated regulation is complex and important for the regulation of more than one inflammatory mediator, (*e.g.* two forms of PLA₂ [Dennis 1994], at least one secreted and one cytosolic). Thus, the role of the PLA₂ in the pathogenesis of inflammatory disease is under scrutiny.

The identities of the specific factor or factors that play pivotal roles in the expression of sPLA₂ from synoviocytes with the progression of rheumatic disease are unknown. sPLA₂ release can be induced by cytokines [Crowl 1991]. Transcriptional inactivators, like actinomycin D inhibit this stimulation. Forskolin, an activator of adenylate cyclase, and modulators of G-protein cascade will mimic the stimulation seen with cytokines like IL-1 β and TNF α [Mochan 1989]. Olivier *et al.* [1994] have shown that there are specific responsive elements, both inhibitory and

stimulatory, in the promoter of the gene in liver extracts, and these elements are sensitive to IL-6, a cytokine associated with sepsis.

1.2 The Diseased Synovium

1.2.1 Clinical Diagnosis

The major criteria for diagnosing rheumatoid arthritis (RA) are as follows: 1) Accumulation of fluid and immune cells within the synovium of the affected joint(s). 2) Synovial hyperplasia. 3) Increase in apparent vascularity through pannus formation. An increase in synovial pressure from sub- to superatmospheric and a marked hypoxia of the pannus tissues due to reperfusion failure are secondary to the fluid accumulation within the synovial cavity [Farrell 1992, Blake 1994]. The pannus is composed of proliferating synovial fibroblasts, macrophages, and angiogenic endothelial cells. These cells have an altered phenotype, leading to their proliferative state.

The Rheumatoid Joint

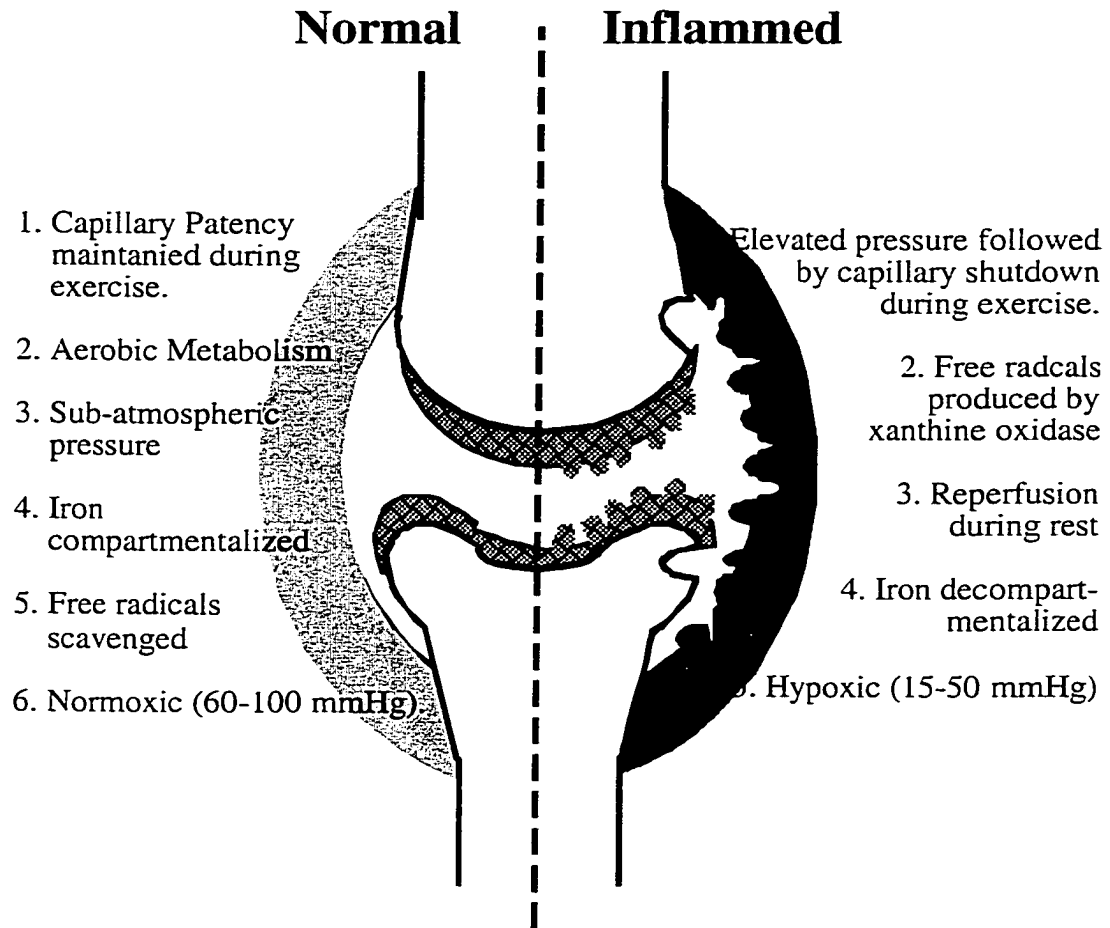


Figure 1. The Rheumatoid Joint: Comparison of healthy (Left) and diseased (Right) synovial tissue.

1.2.2 Cellular Morphology

There are a few criteria to identify transformed rheumatoid synoviocytes from normal fibroblasts [Pruzanski1995]. The first of these characteristics is an increased proliferative state. There are often marked differences in the shape and secretory capacities of the fibroblasts in regions of connective tissue disease. Shape changes in the synovial fibroblasts include the deviation from the typical spindle shape toward a stellate synoviocyte. However, this may not always be observable *in vitro*. Another notable difference between the typical histological phenotype of normal human lung fibroblasts and rheumatoid fibroblasts is the apparent lack of contact inhibition of the latter in culture. When cultured in serum containing media, the rheumatoid fibroblasts will overgrow each other forming dense tracts or foci of cells [pers. obsv.]

1.2.3 Altered Gene Expression

Synoviocytes and intact synovial tissue isolated from rheumatoid individuals demonstrate distinctive patterns of gene expression, producing high levels of many cytokines. Several other secreted products are attributed to the altered state of the cells. Rheumatoid fibroblasts also exhibit more receptors for dexamethasone than their quiescent (non-inflamed) synovial counterparts [Damon 1985]. A number of gene products have elevated levels of expression in the diseased synovium.

Collagenase	Stromelysin
High Molecular Wt. PLA ₂ (cPLA ₂)	Low Molecular Wt. PLA ₂ (sPLA ₂)
VCAM-1	Cyclooxygenase II
IL-1 β	IL-8

Table 1. Inflammatory materials induced in rheumatoid cells by the Disease State.

1.2.4 Chemotactic factors

Synovial fibroblasts and whole synovial tissue isolated from rheumatoid patients demonstrate distinctive patterns of gene expression, producing high levels of many cytokines (TNF alpha, IL-1 alpha and beta and GM-CSF) [Ritchlin 1994]. Some cells also appear to release VEGF. Induction of the cytokine IL-8 is then caused by the inflammatory cytokines IL-1 and TNF- α . The IL-8 promoter is regulated by subunits of the NFkB transcription factor, demonstrating another role for this transcription factor in the expression of the inflammatory reaction. [Kunsch 1993]. IL-8 goes on to act as a chemotactic cytokine for T-lymphocytes and neutrophils. NFkB also leads to the increase of PGE₂ in the synovium [Roshak 1996b]. The lipid mediators; PAF, lysophospholipids, arachidonic acid and prostaglandins, are also potent chemoattractants and mitogenic factors in the immunological milieu. For example, 12(R)-Hydroxy-5,8,14(Z,Z,Z)-eicosatrienoic acid (12(R)-HETrE) a p450 metabolite of the eicosanoid 12-HpETE, is known to be a potent

angiogenic factor, stimulating the proliferation of endothelial cells. 12(R)-HETrE also stimulates expression of the AP-1 proto-oncogenes *c-myc*, *c-jun*, and *c-fos*, and produces an increase in the binding activity of NFκB and AP-1 to oligonucleotides, corresponding to their consensus sequences [Laniado-Schwartzman 1994]. That study suggested that 12(R)-HETrE may produce its angiogenic effect through NFκB activation and proto-oncogene expression. The effect was specific to NFκB and to a lesser degree, a variety of other transcription factors.

1.2.5 Adhesion Molecules

One of the noteworthy adhesion molecules in the synovium is vascular cell adhesion molecule-1 (VCAM-1). It is a ligand of the integrin α_4/β_1 . In a recent study, it has been shown that fibroblasts in the synovium express VCAM-1 [Morales-Ducret 1992]. By expressing this adhesion molecule, the authors suggest, the synoviocytes can partition immune cells. Because of such segregation it is possible to explain the enriched distribution

of memory cells in the synovial lining and of neutrophils within the synovial fluid. This phenotypic marker is apparently peculiar to RA synovial fibroblasts and is not observed in RA dermal fibroblasts.

1.2.6 Hydrolytic and Oxidizing Enzymes

Among the enzymes implicated in the pathophysiology of RA are the phospholipases and the proteinases. The PLA₂ enzymes, which include the venom, digestive and immuno-defensive lipases, share a common substrate specificity: selectively hydrolyzing the *sn*-2 acyl-linkage in phospholipids (the major molecular component of cellular lamellae). Through this hydrolytic activity, these enzymes liberate lyso-phospholipids and free fatty acids. Much of the interest in this class of enzyme lies in their ability to liberate the polyunsaturated fatty acid eicosatetraenoic (arachidonic) acid. This, in turn, acts as an inflammatory mediator by being converted into leukotrienes, prostaglandins, thromboxanes and related oxidation products. There are several major classes of the enzyme. Pancreatic and

sPLA₂ are secreted, calcium dependent (mM range) and have no apparent specificity for acyl-chain type or head group [Dennis 1994]. In a mixed unilamellar vesicle assays, these enzyme types will have roughly equal kinetic rates in hydrolysis of phosphatidylcholine and phosphatidylethanolamine with saturated and unsaturated fatty acids in the *sn*-2 position. The pancreatic type fulfills a digestive role, while the sPLA₂ functions in an immunogenic capacity. The cytosolic form (Type IV) has low calcium requirements (μ M range) and apparent substrate specificity [de Carvalho 1993, Glaser 1993, Leslie 1991]. In the synovium, this activity leads to an increase in available arachidonic acid. In several studies it has been shown that the PLA₂ enzymes are the rate-limiting step in the production of eicosanoids. Because of this direct link between the Phospholipases A₂ and inflammatory processes; it is asserted that modulation of these enzymes we can attenuate inflammatory disease states. Hence, this class of enzymes has become the focus of many biochemical and pharmacological studies.

Various reports assign the origin of this pivotal enzyme to hyperplastic synovial fibroblasts and articular chondrocytes [Suffys 1988, Chang 1986]. Others have suggested that the liver may contribute significantly to the accumulation of sPLA₂ to the synovium [Wright 1990]. In this research, both synovial cells and liver cells are used, and are capable of producing sPLA₂ in the presence of the inflammatory cytokine IL-1 β .

The phenotypic changes in fibroblasts associated with the onset of RA are the secretion of various extracellular matrix (ECM) remodeling enzymes. Proteinases, elevated in RA, include the metalloproteinases (MMP). Metalloproteinases are degradative enzymes known to be present in rheumatoid synovium in large amounts, and the tissue degradation caused by these enzymes may be a major component of joint destruction in rheumatoid arthritis. These molecules include collagenases, gelatinases, and stromelysins. By first denaturing and then making collagen soluble, the MMP's can severely impair the structural integrity of

cartilage and bone. This may also cause hypoxic injury to the tissue due to ischemia and reduced reperfusion.

Another crucial process augmenting the inflammatory response during pannus formation is the release of fibroblast-derived prostaglandin E₂ (PGE₂) [Colville-Nash 1992]. Recalling that eicosanoid production follows the action of PLA₂, the generation of PGE₂ is completed by the enzyme cyclooxygenase (COX). There are apparently two forms of this enzyme in some cells. The first class, COX I, and is constitutive and relatively steady state. COX II, however, is transiently induced during mitogenic stimulation. The expression of PGE₂ increases markedly in stimulated rheumatoid fibroblasts [Roshak 1996a] and the major class of COX enzyme contributing to this phenotypic alteration may be COX II.

1.3 Pharmacological Modulation of Rheumatoid Disease

1.3.1 Steroidal Intervention.

The initial observation of reduced incidence of synovitis in rheumatic individuals during pregnancy [Cuchacovich 1987], led to the use of progesterone, prednisolone, cortisol, and dexamethasone in the treatment of synovitis associated with rheumatoid arthritis. However, the use of corticosteroids is fraught with side effects, and even today, decades past the first use of steroids for the treatment of arthritis, an "acceptable" use of steroids for this indication has yet to be determined [Weisman 1995]. Unfortunately, chronic use can cause osteoporosis and immunosuppression. The corticosteroids may induce the lipocortins and non-lipocortin proteins, putative PLA₂ inhibitors [Mukerjee 1992]. The method of action of these molecules, including the antinflammins, uterglobin and lipocortins, is via obstruction of the substrate/enzyme interfacial boundary [Hower 1994].

To determine the specific effect of corticosteroids on the cells implicated in the pathogenesis of inflammatory disease, studies have been completed in rat mesangial cells [Muhl 1992] and human fibroblasts [Damon 1985]. In the cellular studies of mesangial cells, Pfeilschifter *et al.* [1993], were able to demonstrate a dose-dependant, expression-related reduction of IL-1 β -induced sPLA₂ activity with dexamethasone, prednisolone, hydrocortisone and corticosterones, but not with progesterone. Damon *et al.* [1985] were able to demonstrate heightened activation of the inflamed rheumatoid fibroblasts through the measurement of a three-fold increase of PGE₂ release compared to normal synovial fibroblast cells. Further they showed that there was a relationship between the responsiveness of a given cell type to dexamethasone and the abundance of its dexamethasone receptors.

1.3.2 PLA₂ Inhibitors

The search for specific PLA₂ inhibitors has been elusive [Mayer 1996]. The compounds used to modulate type II PLA₂ are diverse. Some are derived from marine sources, as in the case of Scalaradial. Others are from compound banks [Tramposch 1994] and some are from rational drug design projects based upon enzyme and substrate structures [Bennion 1992]. All inhibit in the pM range. Unfortunately, because of problems ranging from bioavailability to toxicity, they have proven to be therapeutically undesirable.

The alkylating agent *p*-bromophenacylbromide (BPB) is a potent inactivator of phospholipases. It has inhibitory activity in both phospholipases C and A [Schutze 1991]. For this reason, BPB has been used to inactivate PLA₂ [Jacobson 1993]. Because of its generalized activity, binding to exposed histidine residues, it is not always useful for the determination of regulatory paths. It has, however, proven helpful to abolish the release of arachidonic

acid from both phosphatidylcholine and diacylglycerol sources *in vitro*.

Manoalide (isolated from the sponge *Luffariella. viriabilis*) is a potent inhibitor of PLA₂ [Glaser 1988]. It works exceptionally well on the venom phospholipases (IC₅₀ 0.01-5μM). The binding site for manoalide in bee venom phospholipase A₂ was later localized and described by drug sequestration studies. Manoalide has a high affinity for the polypeptide fragment Lys-X-X-Lys. The interaction with this sequence results in an irreversible chromophore formation and subsequent enzyme inactivation.

Scalaradiol, isolated from the sponge *Cacospongia mollior*, has a distinct structure resembling sterols. However, its atypical D ring has six members. This PLA₂ inhibitor acts via a two-step process over the course of 15-30 minutes. The inactivation of human synovial PLA₂ is dependent upon both a and b aldehydic groups.

Lipocortin, calpactin and the annexins (from uteroglobin) are protein inhibitors once thought to directly inhibit the action of

PLA₂. The activity of these compounds has been elucidated *in vitro* as substrate sequestration [Flower and Rothwell 1994]. By intercalating into the phospholipid substrata, these molecules interfere with the catalytic binding of PLA₂ to its substrate. Therefore, this class of inhibitor is too general a regulator for biochemical pathway analysis.

1.3.3 Transcriptional regulation

The sequence of the type II PLA₂ and its promoter have been described [Seilhammer 1989]. Recently, the human gene has been localized to 1p35:35.1 [Praml 1995]. Through this groundwork, and taking into account the synovial milieu [Przanski 1995], it is now possible to ask very specific questions about the transcriptional regulation of the type II PLA₂ gene in the synoviocyte. Along these lines, Olivier *et al.* [1994] demonstrated IL-6-controlled positive and negative regulatory elements in the human type II PLA₂ promoter using rat liver extracts. They localized the negative regulatory elements of the promoter at

1614 to -210 (in the region of the promoter 5' to angiotensin acute phase responsive element at -200), and +20 to +806 the 5'UTR containing exon 1. The positive regulatory elements, as determined by CAT-reporter assay in hepatocellular carcinoma (HepG2) cells, were localized to -210 to +20 with some inducible elements further constrained to -210 to -55.

Among the known transcription factor binding sites described by Olivier *et al.* [1994] in the sPLA₂ (type II), promoter were several acute-phase responsive elements that were activated in response to inflammatory stimuli in liver cells. One of these, the NF-IL-6 (C/EBP b-Zip family) binding consensus sequence, was found as a tandem repeat. Other sites including, but not limited to, AP-2 (cAMP-responding family), AP-1 (*c-fos*), HNF3-RE, the relatively ubiquitous Sp I [Bucher 1990] and the consensus site for the zinc finger transcription factors GATA 1-3 are also located in the promoter region of the type II PLA₂ gene..

Several assumptions have been made about the significance of the transcriptional pathway leading to the activation of the type II

PLA₂ gene. Firstly, the activation pathway is complex [Konieczkowski 1993]. There is a complex interplay between stimulatory and regulatory factors [McCord 1995, Pfeilschifter 1993, and Oliver 1994]. Secondly, steroids and other anti-inflammatory compounds have a potential to work in the transcriptional path, but have unfortunate side effects making them therapeutically inadequate [Weisman 1995]. Finally, it is tempting to speculate that a specific transcriptional modulator for sPLA₂ could attenuate the formation of the pannus; or at least diminish its progression by reducing activation of transcription [Pfeilschifter 1993, Konieczkowski 1993].

1.4 Cellular Models of Inflammatory Disease

1.4.1 Synoviocytes

Rheumatoid fibroblasts, synovial fluid cells, chondrocytes and macrophages in and around the pannus tissue of the rheumatoid joint may be involved in the production of type II PLA₂ [Pruzanski 1995]. A great deal of effort has been invested in attempts to determine the importance of rheumatoid fibroblast release of sPLA₂ into the synovium. The rheumatoid synovial fibroblasts and chondrocytes do indeed release type II PLA₂ into its surroundings in vitro [Roshak 1996a, Pruzanski 1995]. This release is inducible with IL-1 β and results in a doubling of sPLA₂ levels over 24 hours in the fibroblast. This inducibility is not observed in the chondrocyte [Pruzanski 1995]

1.4.2 Normal Fibroblasts

Several normal fibroblast cell lines have been studied for their ability to respond to cytokines by producing sPLA₂. TNF α , for

example, is able to induce the activation of PLA₂ only after pretreatment with the transcriptional inhibitor actinomycin D or the translational inhibitor cycloheximide [Hollenback 1992]. In this study, we are not necessarily observing a type II PLA₂, and we are certainly not looking at a transcriptional modulation by TNF α due to the presence of the inhibitors of expression. This example may be an indication of type IV PLA₂ activation. In an earlier study, Solito [1989] suggested that IL-1 β may induce the expression of PLA₂ in normal fibroblasts. However knowledge of the various types of PLA₂'s was limited at the time of that study, and it is unclear whether or not cytosolic PLA₂ (Type IV) was acting under their experimental conditions. However, in sPLA₂-specific ELISA, normal human lung fibroblasts do not appear to respond to IL-1 β -induction by releasing PLA₂ (personal observation). The type IV PLA₂ is activated in some fibroblast types by IL-1 β , lending support to the observation that some induction of PLA₂ may be attributed to type IV, rather than type II PLA₂ in fibroblasts [Hulkower 1992]. In gingival fibroblasts, cells

capable of inflammatory responses, IL- 1 β has been shown to induce the upregulation of sPLA₂ [Shinohara 1992].

1.4.3 HepG2 Cells

Two very important investigations of the mechanism of sPLA₂ activation have been completed in the HepG2 cell line. The first study confirmed the effect of various cytokines on the release of sPLA₂ from these cells [Crowl 1991]. In studies using combinations of the inflammatory cytokines IL-1 β , IL-6 and TNF α , Crowl *et al.* were able to demonstrate the effect of these compounds on the *de novo* synthesis of sPLA₂. The data lend support to the argument that sPLA₂ should be classified as an acute phase protein. In subsequent molecular studies, Olivier *et al.* [1994] were able to dissect the IL-6 inducible and repressible portions of the sPLA₂ promoter. These studies, with the work of Wright *et al.*, [1990], suggest a more decentralized origin of type II sPLA₂ in sepsis, and also, possibly arthritis. Furthermore, it is clear that the inflammatory cytokine IL-1 β , as well as the acute-phase protein activator IL-6 play important roles in the progression of inflammatory responses.

2 Methods

2.1 Cell Culture.

2.1.1 Human Rheumatoid Synovial Fibroblasts

Sterile synovial tissue was obtained during open joint surgery from patients with rheumatoid arthritis: their diagnosis determined according to criteria of The American Rheumatism Society. Within 3 hours of surgery, the synovial tissue was washed 3 times with DPBS. Under sterile conditions, the tissue was then minced using sterile dissection scissors and a scalpel in DPBS with pen/strep and 1mg claustridiopeptidase A per milliliter in a 10 cm petri dish. The tissue fragments were incubated for 4 hours under culture conditions (37°C and 5% CO₂). The cell suspension was then mixed well by aspiration in equal volumes of trypsin and incubated another hour. The cells were then pelleted by centrifugation (400 x g, 10 minutes, room temperature). The pelleted cells were then washed three times in DPBS without Ca²⁺ and Mg²⁺ at room temperature. The final pellet was resuspended

in EMEM containing 10% FCS, 100 units and 100 μ g streptomycin per milliliter. The final mixture was then seeded into two T₇₅ flasks containing a final volume of 12ml of EMEM. After 24 hours, the media was replaced with fresh EMEM, and the cells were passed three times before use (to expand the rheumatoid synovial fibroblasts (RSF) and allow the macrophages to cease metabolic activity). Because of problems resulting in the reversion of fibroblasts from the "altered phenotypic markers" associated with the disease state, *e.g.* rapid proliferation, secretion of PGE₂, elevated collagenase, and VCAM-1 expression [Dayer 1976, Morales-Ducret 1992], only early passage cells (3-9) were used.

2.1.2 HepG2

Hepatocellular carcinoma cells (HepG2) were purchased from ATCC (#HB-8065). The cells were maintained in EMEM containing 10% FBS and pen/strep and split every 3-4 days.

2.2 Hypoxia Studies in Human Rheumatoid Synovial Fibroblasts

Synovial fibroblasts were prepared as described above. Cells from 80%-90% confluent fibroblasts cultures were plated into 24 well culture plates in one ml EMEM at 5×10^4 cells/well. After adding EMEM \pm IL-1 β to wells, plates were transferred to hypoxic (4 to 5 torr ppO₂ atmosphere) or normoxic (140-150 torr ppO₂) incubators. For hypoxia-reoxygenation studies, 24 hour, hypoxic treatment preceded IL-1 β addition. The conditioned media was immediately assayed at the conclusion of the experiment or stored at -20°C until analysis.

2.3 Type II PLA₂ ELISA

The specific human-Type II PLA₂ ELISA uses reagents provided by SmithKline Beecham Pharmaceuticals (King of Prussia, PA).

Approximately 1.5 mg of anti-PLA₂ Mab SK097-1E8.5.2 was equilibrated in biotinylation buffer (100 mM NaB, 150 mM NaCl, pH 8.5) by passage through an equilibrated 5 ml. crosslinked

dextran desalting column (KwikSep™, Pierce). The IgG containing fractions were detected by UV spectrophotometer (A_{280}). The biotinylation reagent was prepared by dissolving 50 mg of EZ-Link™ NHS-LC-Biotin (Succinimidyl-6-(biotinamido)hexanoate, Pierce) in 1 ml of DMF (Dimethyl formamide). The pooled fractions were then incubated with a 5-fold molar excess of the biotinylation reagent on ice for 2-3 hours. The unreacted reagent was then removed by gel filtration on a KwikSep™ column equilibrated in antibody buffer (50 mM Tris-HCl, 0.02% sodium azide, pH 7.4). After determination of protein concentration by the method of Bradford (1976), the antibody buffer was adjusted to 0.1% BSA to stabilize the antibody.

High-binding 96 well microtitre plates (Falcon, # 3228) were coated with 200ng of capture antibody (SK088-3C6.16.2) in 100 μ l/well coating buffer (50mM sodium phosphate, 150mM NaCl, 0.02% sodium azide, pH 7.4) for 18 hours, at 4°C. The plates were then rinsed 3 times with wash buffer (10mM Tris-HCl, 150 mM NaCl, 0.02% sodium azide, 0.05% tween 20, pH 7.4).

After removing the wash buffer by aspiration the wells were incubated with 150 μ l of blocking buffer (1% BSA in 50 mM Tris-HCl, 150 mM NaCl, 0.02% sodium azide, pH 7.4) for 1-2 hours at 37°C.

Phospholipase A₂ standards consisting of serial dilutions from 4 ng/ml to 125 pg/ml of recombinant human Type II PLA₂ dissolved in EMEM were prepared. After 3 washes, 50 μ l of 2 μ g/ml biotinylated sandwich antibody in Assay Buffer (0.5% bovine gamma globulin, 50 mM Tris-HCl, 150 mM NaCl, 0.02%) and 50 μ l of conditioned media, control or standard recombinant humansPLA₂ suspension was added to each well in duplicate. The plate was then incubated for 1 hour at 37°C.

The streptavidin-alkaline phosphatase (Strep-AP) conjugate was prepared by dilution of a stock solution (Amersham RPN 1234) 1:2000 in streptavidin buffer (0.5% bovine gamma globulin, 50 mM Tris-HCl, 0.02% sodium azide, 1 mM MgCl₂, pH 7.4). After washing the plate 3 times, 100 μ l of diluted Strep-AP conjugate

was added to each well and the plate further incubated at 37°C for 30 minutes.

Following a final washing step, 100 μ l of substrate (1 mg/ml p-nitrophenol phosphate, 9.7% dietanolamine, 1 mM MgCl₂, 0.02% sodium azide, pH 9.8) was added to each of the wells. The plate was then incubated for 30 minutes at 37°C. After color development proceeded to approximately 0.8 absorbance units at 412nm (canary yellow), the plate was read on a Molecular Devices Vmax plate reader with a 412nm cutoff filter. The results were analyzed with Softmax™ software.

2.4 PGE₂ ELISA

Prostaglandin E₂ was measured using a commercially available ELISA system (Cayman Chemical, 514010). Briefly, 50 μ l of conditioned media, standard or control was added to the pre-coated wells with 50 μ l of antiserum and 50 μ l of PGE₂ tracer in duplicate. The plates were incubated overnight at room temperature in the dark. The plates were washed 3 times and

200 μ l of Ellman's reagent (acetyl thiocholine and 5,5'-dithio-bis-(2-nitrobenzoic acid)). The PGE₂ tracer, conjugated to electric eel acetylcholinesterase, cleaves acetate from acetylthiocholine. The thiocholine then attacks the disulfide linkage of 5,5'-dithio-bis-(2-nitrobenzoic acid), liberating 5-thio-2-nitrobenzoic acid. This compound has a maximal absorbance at 412 nm which is inversely proportional to the amount of PGE₂ contained in the conditioned media. The plates were read with a Molecular Devices Vmax plate reader. The data was analyzed with Softmax™ software.

2.5 Preparation of Plasmids for CAT Reporter Assay.

Amplification of plasmids was accomplished by transformation of electrocompetent bacteria. ElectroMAX cells, (GibcoBRL, #DH10B) were first grown in LB broth (10 g bacto-tryptone, 5 g bacto-yeast extract, 10 g NaCl) overnight. The cells were then collected by centrifugation (4000 x g, 15 minutes) and washed 3 times in ice-cold 10% glycerol. (It is important to remove all traces of electrolyte from the cell suspension, otherwise the increased

conductivity can cause explosive results in subsequent steps.) The cells were stored in 10% glycerol at 10^{10} cells/ml in aliquots of 25 μ l for up to 6 months at -70°C .

The cells were thawed on ice. Supercoiled plasmid DNA was prepared by ethanol precipitation and resuspension in nuclease-free DI at 2 ng/ μ l. The cells were then prepared by adding 5 μ l (10 ng) of DNA. The cell/DNA solution was then transferred to a pre-chilled electroporation cuvette (BioRad Pulser Cuvette, #165-2089). Using a BioRad Gene Pulser (#165-2102) set at 18 kV/cm, the cells were pulsed once. SOC medium (2% bacto-tryptone, 0.5% bacto-yeast extract, 10 mM NaCl, 2.5 mM KCl, 10 mM MgCl_2 , 10 mM MgSO_4 , 20 mM glucose) was then added to the cuvette immediately and the cells removed for incubation and recovery at 37°C . The cells were then plated on selective medium (LB-Amp agar, 75 $\mu\text{g/ml}$). Resistant colonies were then grown up in LB-Amp broth (50 $\mu\text{g/ml}$).

Plasmids were purified using a commercially available isolation kit (Promega, Wizard™). This procedure uses a modified form of the alkaline lysis method of Birnborn [1979] and Ish-Horowicz (1981). An overnight selective culture of transformed *E. coli* was pelleted by centrifugation (5 000 x g, 10 minutes, room temperature). The pellet was resuspended and lysed by (5 mM EDTA, 50 µg/ml Rnase A, 0.1 N NaOH and 0.5 % SDS). The solution was neutralized with 1 volume of 1.32 M potassium acetate, pH 4.8. The cellular debris was then removed by centrifugation and the plasmid DNA precipitated in the presence of 1 volume of 2-propanol. The DNA was then applied to a silica-based chromatographic support and impurities were removed by ethanol washes. The plasmid DNA was then eluted from the support with 65°C TE (10 mM Tris-HCl, 1 mM EDTA, pH 7.5). Particulate material was removed by filtration across a 0.22 µM filter. The quality of the DNA was determined by electrophoresis in a 1% agarose gel containing ethidium bromide. DNA concentration and purity was determined by spectrophotometry.

Some of the plasmid DNA was sterilized and re-precipitated in the presence of ethanol.

2.6 Transfection of HepG2 cells with sPLA₂ promoter-CAT Constructs.

HepG2 cells were grown to 90% confluency in T₁₇₅ flasks. The cells were then collected by trypsinization. Briefly, the flask was washed with room temperature DPBS to remove any traces of FBS. The cells were then incubated with 10 ml of trypsin. After the cells were suspended, the trypsin was inactivated by the addition of 90 ml of EMEM containing 10% FBS and pen/strep. The cells were evenly suspended by gentle trituration. The cells were plated into 60 mm tissue culture treated petri dishes (Falcon, #3802), at 10⁵ cells/plate, over 18-22 hours. The media was then removed and the cells fed 4 hours before the transfection precipitate was applied.

Sterile, purified plasmids were dissolved in sterile 250 mM CaCl₂ at 37°C (50 µg/ml). Batches of plasmids for 10 or more plates

were prepared by direct scaling in a 50 ml conical centrifuge tube (Corning, #430290). While using an automatic pipetter with a disposable 5 ml pipette to gently bubble the CaCl₂-plasmid solution, an equal volume of 2x HBS (280 mM NaCl, 10 mM KCl, 1.5 mM sodium phosphate (dibasic), 12 mM dextrose, 50 mM HEPES, pH 7.05) was slowly added using a pasture pipette. The Calcium Phosphate-DNA coprecipitate was allowed to form at room temperature for 20 minutes. The precipitate was then resuspended by gently pipetting up and down once before application to the cells.

Using a wide-bore pipette, 500 µl of the DNA precipitate (12.5 µg DNA) was gently added to the medium above the cells. The plate was then gently rocked to distribute the precipitate evenly. The plates were then incubated under culture conditions. After 4 hours, the media was removed and the cells were glycerol shocked (15% glycerol in 1 x HBS) for 30 seconds. Following shock, the dishes were washed 3 times with DPBS. The cells were then fed with 7 ml. of EMEM containing 10% FBS and pen/strep,

and allowed to rest 18 hours. Following this recovery period, the cells were fed once again and drug treatments were begun.

2.7 Chloramphenical Acetyl Transferase ELISA

The expression level of reporter plasmids containing the chloramphenical acetyl transferase gene was quantified using a commercially available ELISA (Boehringer Mannheim, #1363727). Cells grown in 60 mm petri dishes were first washed 3 times with ice-cold DPBS. The cellular membranes were then disrupted with 1 ml of lysis buffer for 30 minutes at room temperature. The cytoplasmic lysate was then collected by pipetting (the nuclei remain attached to the dish). The cellular debris is removed by centrifugation (14 000 g, 10 minutes, 4°C). The protein concentration was then measured using as in Bradford (1976). Protein concentration was adjusted to 250 µg/ml with lysis buffer. To each of the wells of the precoated plate, 200 µl of the various cellular extracts were added in duplicate. The plate was then incubated 1 hour at 37°C. The plates were then washed 3 times

with wash buffer (PBS, Tween 20). To each of the wells, 200 μ l of anti-CAT-DIG (sandwich antibody) was added and incubated for 1 hour at 37°C. The wells were then washed 3 times to remove unbound sandwich antibody. To each of the wells, anti-DIG-POD antibody (2° antibody) was added and incubated for 1 hour at 37°C. The unbound 2° antibody was then removed by 3 successive washes. To detect the presence of 2° antibody, and thus ultimately CAT, 200 μ l of ABTS® substrate was added to each of the wells. Color developed over an hour and was measured by A₄₉₀ on a Molecular Devices Vmax plate reader. The data were analyzed using Softmax™ software.

2.8 Electrophoretic Mobility Shift Assay (EMSA)

These assays were performed on nuclear extracts from HepG2 cells that had been subjected to drug treatment and IL-1 β . Nuclear extracts were prepared according to Dingam [1983]. Approximately 10⁷ cells were grown to 80% confluency in EMEM with 10% FBS and pen/strep. These cells were then incubated

with drug at 1 $\mu\text{g}/\text{ml}$ for one hour. The cells were then exposed to IL-1 β (400 ng/ml) for 1-8 hours. The cells were then trypsinized, pelleted by centrifugation (400 x g, 10 minutes, room temperature), and washed three times with ice-cold DPBS. The cell pellet was then resuspended in 20 μl of hypotonic Buffer A (10 mM HEPES, 10 mM KCl, 1.5 mM MgCl₂, 0.5 mM DTT, 0.1% NP-40, pH 7.9) for 10 minutes on ice. The nuclei were then collected by centrifugation at 3500 rpm (1200 x g) in an Eppendorf microfuge for 10 minutes at 4°C. The supernatant (cytosolic fraction) was discarded, and the nuclei were resuspended in 15 μl of high salt Buffer C (20 mM HEPES, 420 mM NaCl, 1.5 mM MgCl₂, 25% glycerol, 0.2 mM EDTA, 0.5 mM DTT, 0.5 mM PMSF, pH 7.9). This suspension was then subjected to three 10-second sonication pulses (microprobe dismembrator, 30%, Fisher). The suspension was then allowed to incubate 20 minutes on ice with gentle shaking. The nuclear debris was then collected by centrifugation (12 000 x g, 10 minutes, 4°C). The supernatant containing the nuclear extract was then diluted to 75 μl with buffer D (20 mM

Hepes, 50 mM KCl, 20% glycerol, 0.2 mM EDTA, 0.5 mM DTT, 0.5 mM PMSF, pH 7.9). The protein concentration of the nuclear extract was determined as in Bradford and then stored at -70°C.

Consensus oligonucleotides were purchased from Promega (Madison, WI). Following manufacturer's recommendations, the labeling reactions were assembled as in Table 2.

Consensus Oligonucleotide (1.75 pmol/ μ l)	2 μ l
10x T4 Polynucleotide Kinase Buffer	1 μ l
[γ - ³² P]ATP (Amersham, Redivue #AA0018)	1 μ l
Nuclease-Free Water	5 μ l
T4 Polynucleotide Kinase (10 U/ μ l)	1 μ l

Table 2. Electrophoretic Mobility Shift Assay Labeling Reaction.

The reaction was then incubated for 10 minutes at 37°C and was terminated by the addition of 1 μ l of nuclease-free EDTA. The volume was then adjusted to 100 μ l with TE buffer. Labeled probes were stored for up to 30 hours at 4°C before use.

For each EMSA, 4 separate reactions were prepared. The components of each are shown in Table 3.

Reaction #1 (Negative Control)		Reaction #2 (Positive Control)	
Nuclease-Free Water	7 μ l	Nuclease-Free Water	5 μ l
5x Gel Shift Binding Buffer	2 μ l	5x Gel Shift Binding Buffer	2 μ l
		Nuclear Extract (10 μ g)	2 μ l
Reaction #3 (Specific Oligo.)		Reaction #4 (Nonspecific Oligo.)	
Nuclease-Free Water	4 μ l	Nuclease-Free Water	4 μ l
5x Gel Shift Binding Buffer	2 μ l	5x Gel Shift Binding Buffer	2 μ l
Nuclear Extract (10 μ g)	2 μ l	Nuclear Extract (10 μ g)	2 μ l
Unlabeled Consensus Oligo. (20x)	1 μ l	Unlabeled Consensus Oligo. (20x)	1 μ l

Table 3. Labeling reactions for nuclear extracts.

Each of these reactions was incubated at room temperature for 10 minutes before addition of 1 μ l of [γ - 32 P]ATP-labeled oligonucleotide. The reaction tubes were then incubated at room temperature for an additional 20 minutes. Non-denaturing gel-loading buffer (1 μ l, 250 mM Tris-HCl, 0.2% bromophenol blue, 40% glycerol, pH 7.5) was added to each tube immediately before electrophoresis.

5x TBE (54 g Tris base, 27.5 boric acid, 20 ml 0.5 mM EDTA) 8 ml

30% Acrylamide Stock (37.5:1)	6 ml
50% Glycerol	2 ml
30% Ammonium Persulfate	100 μ l
TEMED	14 μ l
DEPC-Treated Water	
	40 ml

Table 4. Slab gels (16 cm x 10 cm x 0.75 mm) were prepared by combining the above reagents.

After 2 hours, the gels were pre-run at 150V for 60 minutes in 0.5x TBE. Samples were then applied to the gel and electrophoresis was carried out at continuous 35 mA until the

bromophenol blue in the sample buffer had migrated 2/3 of the length of the gel. The gel was then transferred to Watman #1 paper and dried for 2 hours at 80°C. Gels were visualized with Kodak BioMax® MS autoradiography film after exposure overnight at -70°C in an 8" x 10" autoradiography cassette equipped with intensifying screens (Fisher, #FB-IS-810).

2.9 Bioassay-Guided Marine Natural Product Studies

A major limiting factor for these studies was a shortage of supply to fully investigate the mechanism of action. The experiments concluded after the supply of extracts were exhausted. Furthermore, the types of experiments were controlled by this shortage. *Ceratodictyon* and *Lyngbya* extracts were only available in small amounts (less than 5 mg total, including crude fractions). This fact limited the type of experiments that could be completed. Animal studies were not possible, nor were replicates of EMSA assays. Therefore, to gain the greatest amount of information from the least amount of compound, the following

strategy was adopted: Cells were prepared for compound study by plating 1:4 from T₁₇₅ culture flasks into 24-well tissue culture plates. After 24 hours, the medium in each of the 24 wells was replaced with 1 ml of EMEM containing 1% ITSS (Insulin, Transferrin, Selenium Supplement, BRL #51300) and pen/strep. Drugs were prepared by dissolution in 100% HPLC-grade methanol. The methanol/drug solution was then aliquoted into clean two-dram vials. The methanol was then removed under a stream of nitrogen. The film of drug in the vial was then re-dissolved in DMSO (1 mg/ml). For studies involving 1° crude extracts, a final culture concentration of 25 µg/ml (2.5% DMSO) was used. For 2° crudes, first level of purification, 10 µg/ml (1% DMSO) was used. For all subsequent screening studies, 1 µg/ml (1% DMSO) was used. After a 1 hour compound incubation, the medium in each of the treatment wells was replaced with EMEM containing 10% FBS and pen/strep containing 400 pg/ml IL-1β (Genzyme, #80-3542-01) and incubated for 24-26 hours. At the end of the IL-1β treatment, the cells were examined under an

inverted microscope (Nikon, Model 500) for signs of cytotoxicity. The conditioned medium was frozen at -20°C for further analysis.

2.10 LDH Release Assay

Using a commercially available assay (Promega, CytoTox), the amount of cytotoxicity for compounds was calculated. This assay is based upon observation that cellular impairment leads to the spontaneous release of lactose dehydrogenase. Lactate is oxidized to pyruvate in the presence of the electron acceptor NAD^+ by this enzyme. In the presence of NADH, the CytoTox substrate is converted into formazan. HepG2 cells were plated at 500 cells / well in 96 well culture plates (Falcon, #3072). Drugs were prepared by diluting stock solutions (1 mg/ml in DMSO) at 1 $\mu\text{g}/\text{ml}$ in EMEM containing 10% FBS and pen/strep. In quadruplicate, 250 μl of the extract/media solution was added to the wells. The plates were incubated under culture conditions for 24 hours. LDH release was quantified as the relative amount of LDH released into the medium versus total cellular LDH.

Comparisons were made between compound and control treatments.

2.11 MTT Mitochondrial Viability Assay

HepG2 cells were plated at 500 cells / well in 96 well culture plates (Falcon, #3072). Extracts were prepared by diluting stock solutions (1 mg/ml in DMSO) at 1 µg/ml in EMEM containing 10% FBS and pen/strep. In quadruplicate, 250 µl of the drug/media solution was added to the wells. The plates were incubated under culture conditions for 24 hours. The medium in each of the wells was then removed and replaced with 100 µl of EMEM containing 5 µg of MTT reagent ((3-[4,5-Dimethylthiazol-2yl]-2,5-Diphenyltetrazolium Bromide). The plates were then incubated under culture conditions for 3 hours. To terminate the reaction, lyse the cells and solubilize the formazan dye, 150 µl of HCl:2-propanol (2:580) was added to each well. The plates were then read using a Molecular Devices Vmax plate reader using a dual

beam (570nm – 590nm) to subtract background absorbance at 590nm.

2.12 Sea Urchin Embryo Assay

Strongylocentrotus purpuratus eggs and sperm were collected in filtered raw sea water. Spawning was induced by injection of 3-5 ml. of 0.5 M KCl periorally. The eggs were prepared by passing 3 times through a 150 μ M nylon mesh. The eggs were then centrifuged in an IEC clinical centrifuge for 4 minutes on the lowest setting (approximately 200 rpm). The packed eggs were then resuspended a 1% (v/v). The sperm were prepared by careful collection from the aboral surface with a clean pasture pipette. The sperm were then stored on ice for up to 10 minutes. Immediately before fertilization, 5 drops of concentrated sperm were diluted in 5 ml. of filtered seawater. Drugs (10 μ g in 10 μ l of DMSO) were added to 29 x 80 mm glass shell vials and equilibrated to 15°C in a shaking water bath. To each 100 ml suspension of eggs, 1 ml of diluted sperm was added and allowed

to incubate for 1 minute at 15 °C. The fertilized cells were then added to each shell vial (1 ml / vial in duplicate). The progress of cell division was monitored by light microscopy of vehicle treated cells. After approximately 2.5 hours, control cells have undergone their first mitotic division, and within 4 hours greater than 95% of control embryos completed the second division. Drug treated cells were compared to control cells at both 2 and 4 cell checkpoints.

2.13 Purified Microtubule Complex Interference

Tubulin, purified from beef brain, [Panda 1995] was thawed and centrifuged. The tubulin (1.5 mg/ml) was mixed with *Strongylocentrotus purpuratus* flagellar seeds in PMMEG buffer (87 mM Pipes, 36 mM Mes, 1.4 mM MgCl₂, 1 mM EGTA and 1mM GTP, pH 6.8), and incubated at 36°C in the presence of purified kalkitoxin. After 20-25 minutes, the formation of polymers was compared to control levels (in the presence of vehicle controls) using semi-quantitative techniques. Briefly, using a video microscope, the number and relative size of microtubules present

in the reaction mixture was noted as a percentage of inhibition of microtubule polymerization.

3 Results

3.1 Cellular Models

3.1.1 Rheumatoid Fibroblasts

In the initial phases of the investigation, the rheumatoid fibroblasts were examined for the expression of several phenotypic markers associated with the hallmarks of the disease. In the synovium, hypoxia/reperfusion cycles often predominate [Blake 1994], and inflammatory cytokines are sometimes at elevated levels [Mizel 1981]. To examine the significance of these factors on the expression of disease markers, both hypoxia and IL-1 β were tested on isolated synoviocytes. Normal human lung fibroblasts (NHLF) were used as controls.

Using both hypoxic and IL-1 β -induced models (10 ng/ml), the expression of PGE₂ was measured for several rheumatoid donors. There was a time dependant increase in the expression of PGE₂ secretion, over the 48hours t of IL-1 β treatment. Hypoxia was not able to induce an increase in PGE₂ secretion greater than two-

fold. However, IL-1 β was able to induce such an increase. The combination of IL-1 β and hypoxia together were additive as can be seen below.

Rheumatoid Synovial Fibroblast-derived PGE₂ with hypoxic and Interleukin-1 β stimuli.

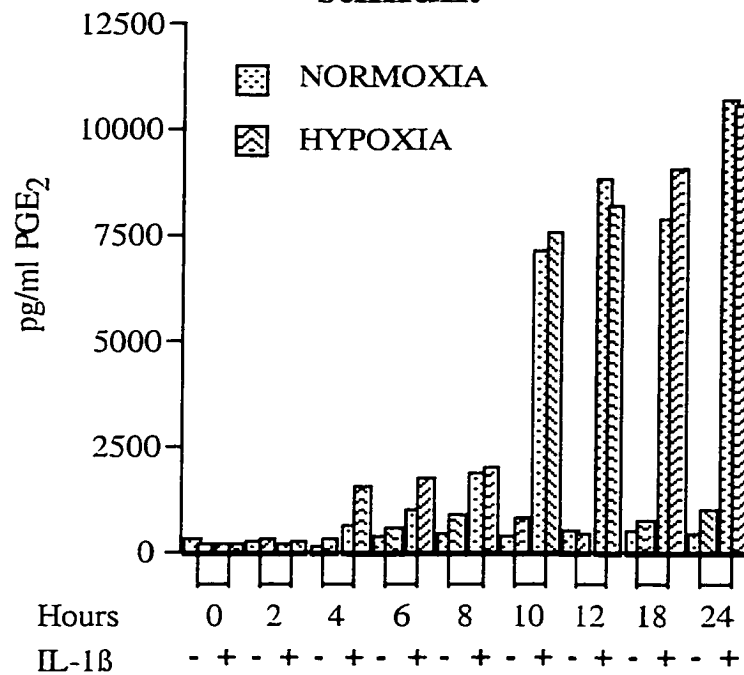


Figure 2. RSF-Derived PGE₂ after 24 hours of incubation in a hypoxic chamber \pm IL-1 β (10 ng/ml). N=3.

Experiments examining the effect of IL-1 β on the secretion of type II PLA₂ are compiled below. Maximal sPLA₂ secretion is observed after approximately 48 hours. A detectable difference between treatment and control groups is observed within 24 hours at doses as low as 100 pg/ml IL-1 β .

RSF IL-1 β Dose Curve

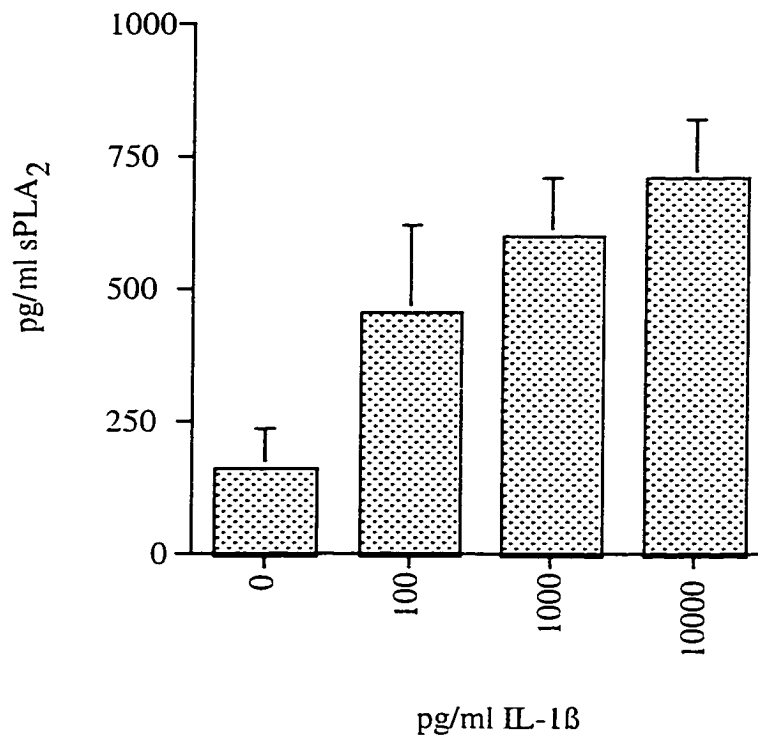


Figure 3. Dose- Response (PGE_2 production) of IL-1 β on cultured Rheumatoid Synovial Fibroblasts (RSF) over 24 hours. Error bars represent one standard deviation, N=3.

After completing a dose-response study of rheumatoid fibroblasts in passages 3 through 11, the optimal IL-1 β concentration and exposure was 10 ng/ml • 24 hours of treatment

Rheumatoid Synovial Fibroblast-derived sPLA₂ time course

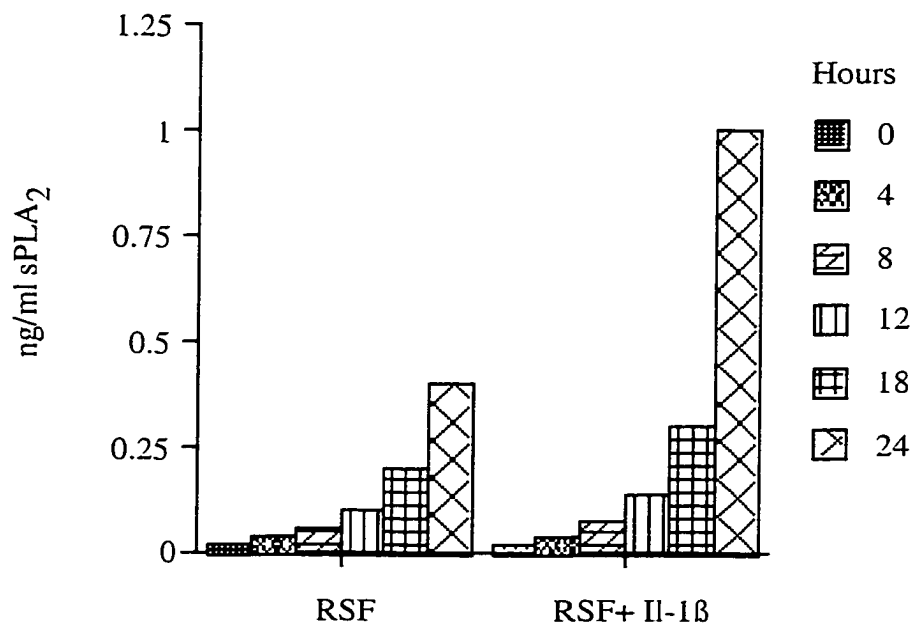


Figure 4. The effect of IL-1 β on the secretion of PLA₂ from RSF over 24 hours. N=3.

3.1.2 Normal Human Lung Fibroblasts

In control experiments, the NHLF cells did not respond to hypoxia and/or IL-1 β in a manner consistent with that observed in the synoviocytes. This is summarized in Figure 5 below.

Effect of Hypoxic Conditions on the Production of PGE₂

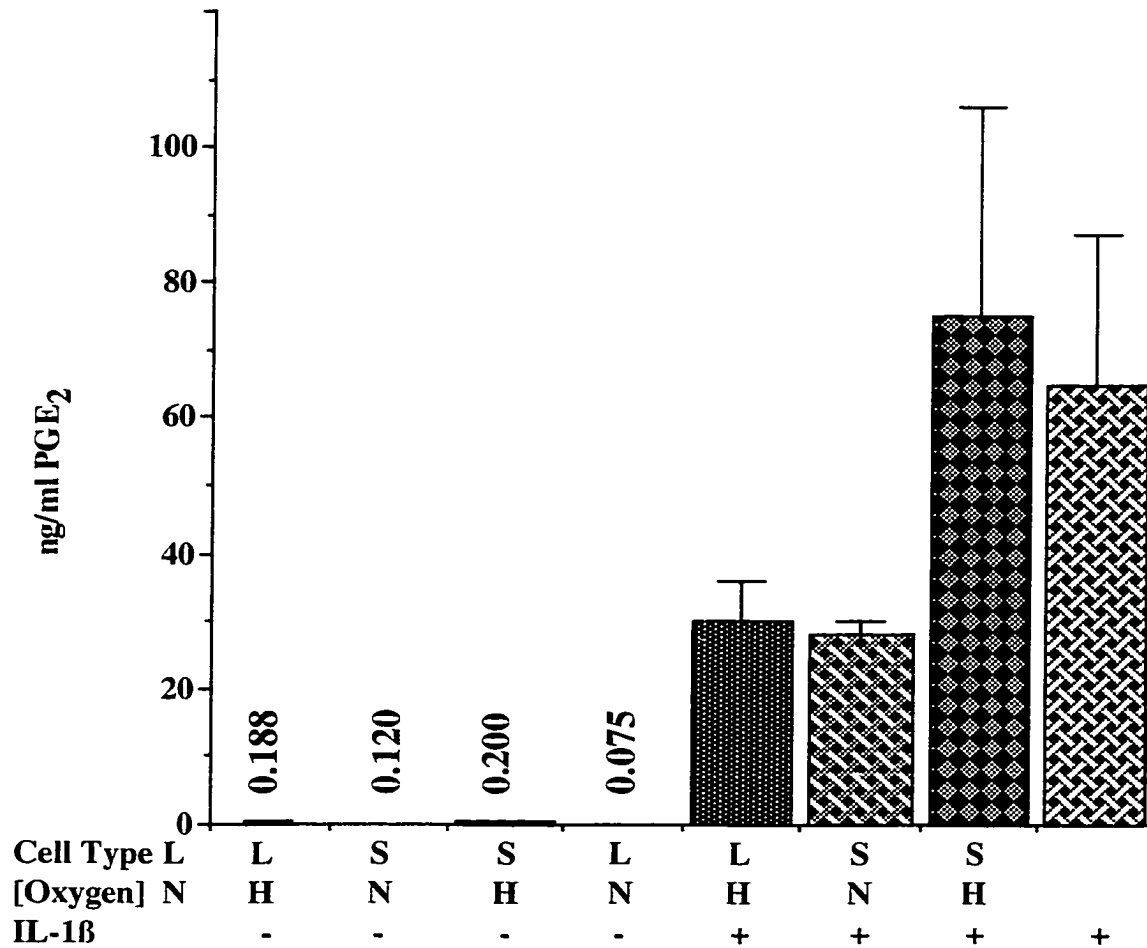


Figure 5. A study of the effect of hypoxia (H), normoxia (N) and IL-1 β (1 ng/ml) on RSF (S) and NHLF (L) -derived PGE₂. Error bars represent one standard deviation, N=12.

Hypoxia and IL-1 β have differential effects on the two cell fibroblast types used. The level of normal fibroblast-derived, IL-1 β -induced PGE₂ differs markedly from that of the rheumatoid synoviocytes (Figure 2, Figure 4). Secreted PLA₂, is undetectable in NHLF, in contrast to the levels detected from cultured, transformed synovial fibroblasts. The data from these preliminary studies was used to develop a more congruent model to guide the fractionation of potentially anti-inflammatory compounds in the marine natural product bank. IL-1 β -induced PGE₂ and sPLA₂ release were developed for further study in the fibroblasts, and later, HepG2 cells.

3.1.3 HepG2 Cells

The Hepatocellular carcinoma cells have been shown elsewhere [Crowl 91] to express secreted PLA₂ in response to IL-1 β , IL-6 and TNF- α (Figure 6).

HepG2 Cytokine Data

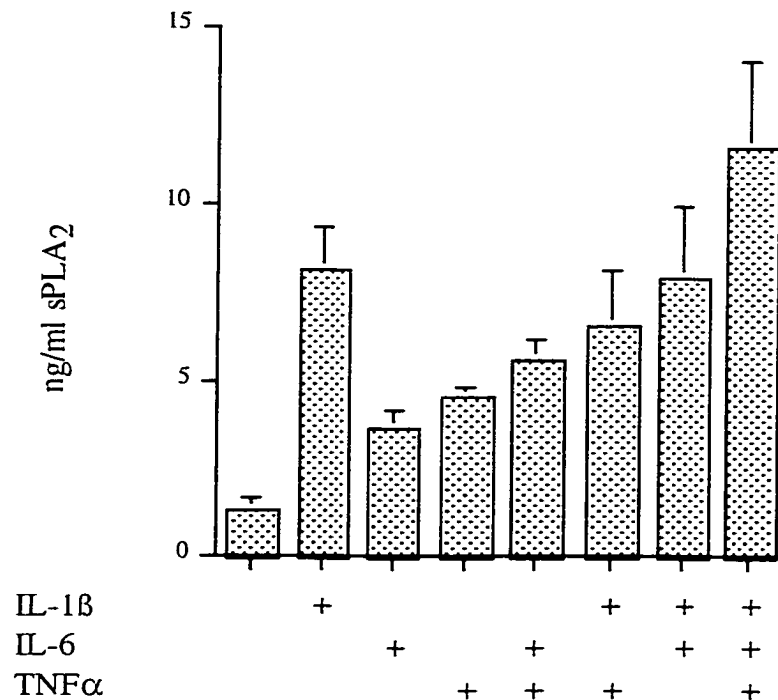


Figure 6. The effects of pro-inflammatory cytokines on the expression of sPLA₂ in HepG2 cells over 48 hours. Error bars represent one standard deviation, N=8.

In studies of the Hepatocellular carcinoma cells, IL-1 β responses were as per RSF studies. The secretion of sPLA₂ was a time dependant process under the influence of IL-1 β (Figure 8).

Time course of secreted PLA₂ production by IL-1 β stimulated HepG2 cells

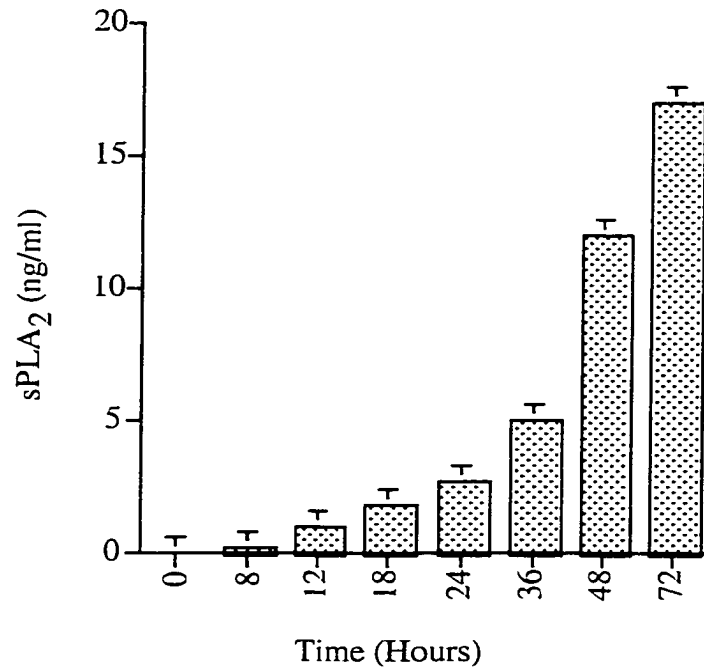


Figure 7. Effect of human-IL-1 β (400 pg/ml) on HepG2 cells over time. Error expressed as one standard deviation, N=6.

HepG2 IL-1 β Dose Response Curve

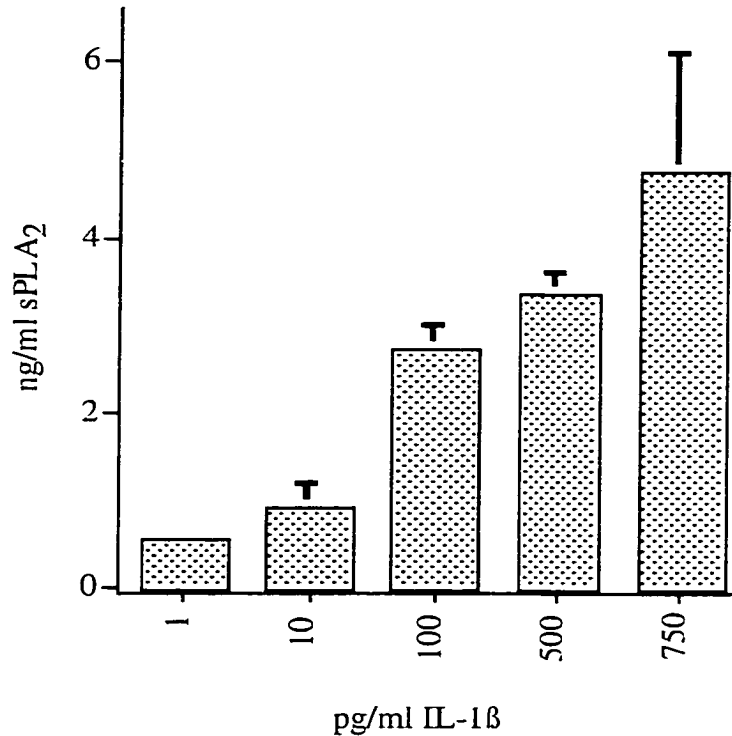


Figure 8. The effect of increasing concentration of IL-1 β on HepG2 cells over a 24-hour period. Error bars represent one standard deviation, N=12.

Maximum response was seen after 48 hours of IL-1 β treatment. IL-1 β has an EC₅₀ for sPLA₂ production, in HepG2 cells, of 400 pg/ml•24 hours. Under standard conditions (400 pg/ml IL-1 β , 24 hours), the model is sensitive to several anti-inflammatory drugs

and molecular tools directed at gene expression. These compounds and their effects are below shown in Table 5.

Drug	Concentration	Site of Action	Inhibition
Dexamethasone	(1 μ M)	Lipocortin Promoter	66%
Cycloheximide	(1 μ g/ml)	Protein Synthesis Inhibitor	74%
Curacin A	(100nM)	Microskeletal Destabilizer	100%
Vinblastine	(10 μ M)	Microskeletal Destabilizer	75%
Zileuton	(1 μ g/ml)	5-Lipoxygenase Inhibitor	0%
Indomethacin	(500 μ M)	Cyclooxygenase Inhibitor	16%
Pseudopterosin A	(10 μ M)	PLA ₂ Inhibitor	5%
KN62	(100 μ M)	Ca ²⁺ -Dependant Kinase Inhibitor	-1%
H89	(100 μ M)	Protein Kinase A Inhibitor	11%
Staurosporine	(2 μ M)	Ser/Thr Kinase Inhibitor	-265%
Bay 11-7082	(1 μ g/ml)	I κ B- α Kinase Inhibitor	40%
Bay 11-7085	(1 μ g/ml)	I κ B- α Kinase Inhibitor	12%

Table 5. The table above represents the effects of drugs having inhibitory effects at various points of the inflammatory cascade as observed in HepG2 cells, N=6.

3.2 Bioassay-Guided fractionation

Having established the response of the cell line to anti-inflammatory attenuation, a series of studies were performed on marine extracts from invertebrate, plant and cyanobacterial sources. The subsequent fractionation was carried out by researchers at the Oregon State University, College of Pharmacy. The preliminary bioassay results are presented in Table 6.

Designation	Origin		% Inhibition
WG1	<i>Udotea</i>	sp	85.72
WG2	<i>Acetabularia</i>	sp	63.56
WG3	<i>Agarum</i>	<i>cribosum</i>	50.67
WG5	Stony globose coral		48.58
WG6	Blue Green algae (BGA) coral killer		50.33
WG7	<i>Laurencia</i>	sp	51.80
WG8	<i>Porteria</i>	<i>homananni</i>	96.35
WG9	<i>Neoptilota</i>	<i>asplenoides</i>	78.10
WG10	Yellow microalga		62.71
WG11	<i>Sargassum</i>	<i>thumbergii</i>	44.98
WG13	<i>Bryopsis</i>	sp	70.61
WG15	<i>Gracillaria-like alga</i>		64.07
WG18	Mat BGA		49.61
WG19	Red Corraline alga		50.38
WG22	Spherical Corraline alga		63.88
WG25	<i>Siphonocladus</i>	sp	41.65
WG29	<i>Dictyota</i>	sp	38.12
WG33	<i>Batrachyospermum</i>	sp	58.53

WG46	<i>Corallina</i>	sp	50.90
WG47	Yellow hair-like alga		34.17
WG51	<i>Turbinaria</i>	<i>ornata</i>	43.54
WG52	<i>Pteroccludia</i>	sp	53.68
WG61	<i>Dictyota</i>	sp	35.74
WG67	BGA		25.53
WG86	<i>Laurencia</i>	<i>doitii</i>	91.07
WG89	<i>Bastrychia</i>	sp	61.21
WG93	<i>Rhodophyta</i>	sp	82.87
WG163	<i>Rhodymenia</i>	<i>pertusa</i>	0.00
WG164	<i>Acrosiphonia</i>	<i>coalita</i>	0.00
WG295	<i>Laminaria</i>	<i>sinclairii</i>	26.83
WG428	<i>Dictyota</i>	sp	10.81
WG443	<i>Galaxaura</i>	<i>subvertacilliata</i>	12.82
WG472	<i>Codium</i>	sp	0.00
WG473	<i>Gracillaria</i>	sp	0.00
WG497	<i>Laurencia</i>	sp	77.57
WG502	<i>Dictyota</i>	sp	49.61
WG566	<i>Laurencia</i>	sp	77.41
WG576	<i>Halimeda</i>	<i>opunita</i>	71.93
WG579	<i>Galaxaura</i>	<i>marginata</i>	90.05
WG584	<i>Heterosiphonia</i>	sp	0.00
WG641	<i>Lyngbya</i>	sp	28.19
WG642	<i>Lyngbya</i>	<i>majuscula</i>	0.00
WG658	<i>Lyngbya</i>	<i>majuscula</i>	0.00
WG659	<i>Egregia</i>	<i>menzesii</i>	0.00
WG664	<i>Lyngbya</i>	sp	0.00
WG725	<i>Zellera</i>	sp	0.00
WG738	BGA		0.00
WG749	<i>Lyngbya</i>	sp	77.57
WG772	<i>Lyngbya</i>	sp	49.61
WG773	<i>Lyngbya</i>	sp	90.00
WG774	<i>Lyngbya</i>	sp	77.41
WG775	<i>Symploca</i>	sp	71.93
WG778	<i>Halimeda</i>	<i>monile</i>	90.05
WG781	<i>Tunicate</i>		20.33

WG783	unk.		100.00
WG784	<i>Rhodophyta</i>		6.45
WG802	<i>Laurencia</i>	<i>sp</i>	62.01
WG818	<i>Halimeda</i>	<i>sp</i>	65.41
WG829	<i>Gracillaria</i>	<i>sp</i>	5.65
WG831	<i>Lyngbya</i>	<i>majuscula</i>	43.87
WG842	<i>Lyngbya</i>	<i>majuscula</i>	20.24
WG845	<i>Rhodophyta</i>		93.67
WG846	<i>Chlorodemsis</i>	<i>fastigila</i>	67.76
WG849	<i>Chlorophyta</i>		58.61
WG851	<i>Ceratodictyon</i>	<i>spongiosum</i>	84.21
WG853	<i>Linosicum</i>	<i>patella</i>	27.55
WG854	<i>Acetabularia</i>	<i>sp</i>	82.18
WG891	<i>Dictyota</i>	<i>sp</i>	0.00
WG894	<i>Lyngbya</i>	<i>aestuarii</i>	7.50
WG895	<i>Avrainvillea</i>	<i>longicalus</i>	32.54
WG896	<i>Dictyota</i>	<i>sp</i>	26.91
WG903	<i>Dictyota</i>	<i>jamaiceasis</i>	36.41
WG906	<i>Lyngbya</i>	<i>sp</i>	28.52
WG908	<i>Lyngbya</i>	<i>sp</i>	51.11
WG909	<i>Dictyota</i>	<i>dichomata</i>	87.16
WG910	<i>Green tufts</i>		84.33
WG919	<i>Lyngbya</i>	<i>majuscula</i>	56.55
WG920	<i>Lyngbya</i>	<i>majuscula</i>	50.23
WG921	<i>Lyngbya</i>	<i>majuscula</i>	42.58
WG925	BGA		84.11
WG927	<i>Lyngbya</i>	<i>majuscula</i>	46.04
WG929	<i>Lyngbya</i>	<i>majuscula</i>	15.87
WG930	<i>Lyngbya</i>	<i>majuscula</i>	0.00
WG931	<i>Lyngbya</i>	<i>majuscula</i>	30.71
WG933	<i>Lyngbya</i>	<i>majuscula</i>	92.85
WG934	<i>Lyngbya</i>	<i>majuscula</i>	82.67
WG941	<i>Lyngbya</i>	<i>sp</i>	78.14
WG947	<i>Avrainvillea</i>	<i>isarafolia</i>	89.75
WG948	<i>Lyngbya</i>	<i>sp</i>	90.29
WG949	<i>Lyngbya</i>	<i>sp</i>	76.13

WG950	<i>Schizothrix</i>	<i>sp</i>	71.54
WG952	<i>Sargassum</i>	<i>sp</i>	65.54
WG956	<i>Galaxaura</i>	<i>sp</i>	100.00
WG958	<i>Lyngbya</i>	<i>sp</i>	100.00
WG961	<i>Lyngbya</i>	<i>sp</i>	62.13
WG962	<i>Lyngbya</i>	<i>sp</i>	65.32
WG963	<i>Lyngbya</i>	<i>sp</i>	75.50
WG964	<i>Phaeophyta</i>		57.86
WG965	<i>Lyngbya</i>	<i>sp</i>	77.47
WG966	<i>Lyngbya</i>	<i>sp</i>	81.58
WG967	<i>Schizothrix</i>	<i>Sp</i>	63.27
WG970	<i>Laurencia</i>	<i>sp</i>	60.75
WG972	<i>Spahacelaris</i>	<i>Novae-hollandiae</i>	81.81
WG973	<i>Lyngbya</i>	<i>sp</i>	76.16
WG974	<i>Lyngbya</i>	<i>sp</i>	79.00
WG975	<i>Lyngbya</i>	<i>sp</i>	85.11
WG976	<i>Lyngbya</i>	<i>sp</i>	63.90
WG977	BGA carpet		61.86
WG997	Unk		54.83
WG998	<i>Caulerpa</i>	<i>Racemosa</i>	66.20
WG999	<i>Centroceras</i>	<i>Clavulatum</i>	58.96
WG1000	<i>Bryopsis</i>	<i>sp</i>	82.33
WG1001	<i>Agardiella</i>	<i>Subulata</i>	38.94
WG1002	Alga		84.30
WG1003	Alga		35.98
WG1005	Alga		45.73
WG1006	Alga		77.56
WG1007	Alga		44.72
WG1008	Alga		91.69
WGAGD	Alga		46.12
WG911	Green tufts		34.15
WG912	<i>Avrainvillea</i>	<i>Rawsonii</i>	84.83
WG913	BGA		70.77
WG914	Red <i>Lyngbya</i>	<i>sp</i>	34.15

Table 6. Preliminary bioassay of various marine extracts in the HepG2 model of inflammation. Columns represent the chemist's designation, Phylum, Genus and species (if available), and percent inhibition of sPLA₂ secretion in the model (N≥6).

Further bioassay-guided fractionation provided additional data for active (≥ 75% inhibition) crude extracts showing less than 100 mAU increase in the MTT assay. The extracts which were active, low in mitochondrial toxicity and abundant enough (> 5 mg) for further study were WG- 773, 778, 845, 851, 854, 933, 947, 956 and 975 (Figure 9-Figure 17).

WG-773 Primary Fractions

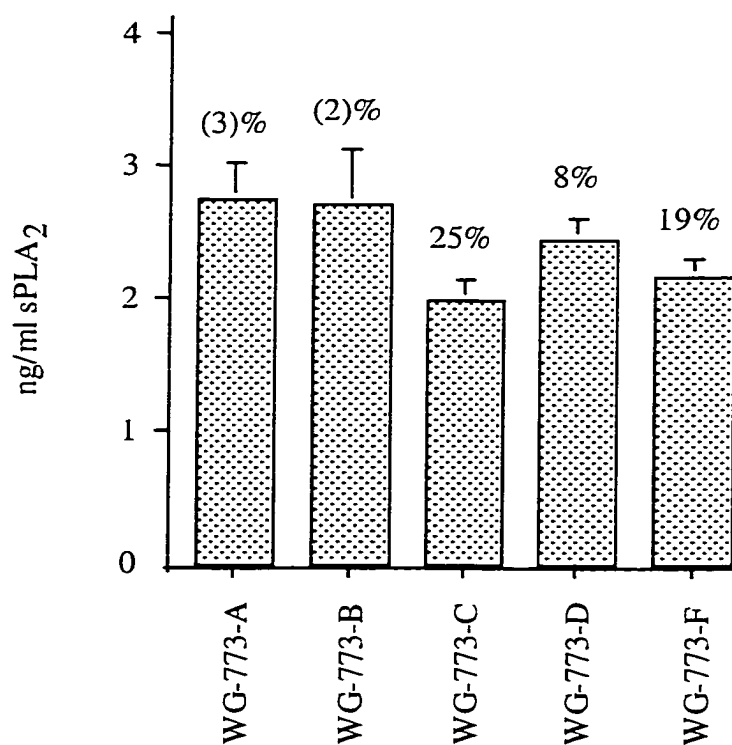


Figure 9. Comparison of the biological activity from the first round of fractionation in the HepG2 model of inflammation. Error expressed as one standard deviation, Numbers represent % inhibition, parentheses > 100% stimulation, N=6.

WG-778 Primary Fractions

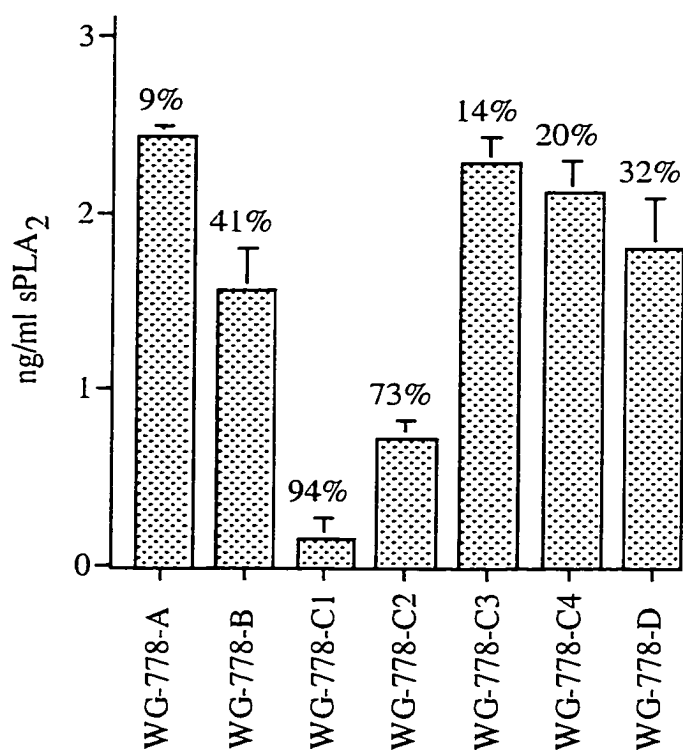


Figure 10. Comparison of the biological activity from the first round of fractionation in the HepG2 model of inflammation. Error expressed as one standard deviation, Numbers represent % inhibition, parentheses > 100% stimulation, N=6.

WG-845 Primary Fractions

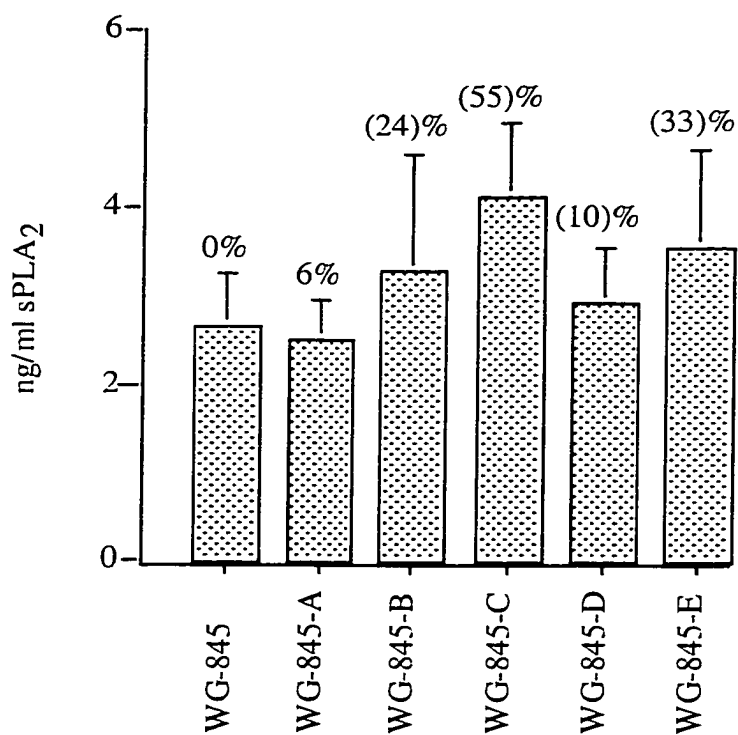


Figure 11. Comparison of the biological activity from the first round of fractionation in the HepG2 model of inflammation. Error expressed as one standard deviation, Numbers represent % inhibition, parentheses > 100% stimulation, N=6.

WG-851 Primary Fractions

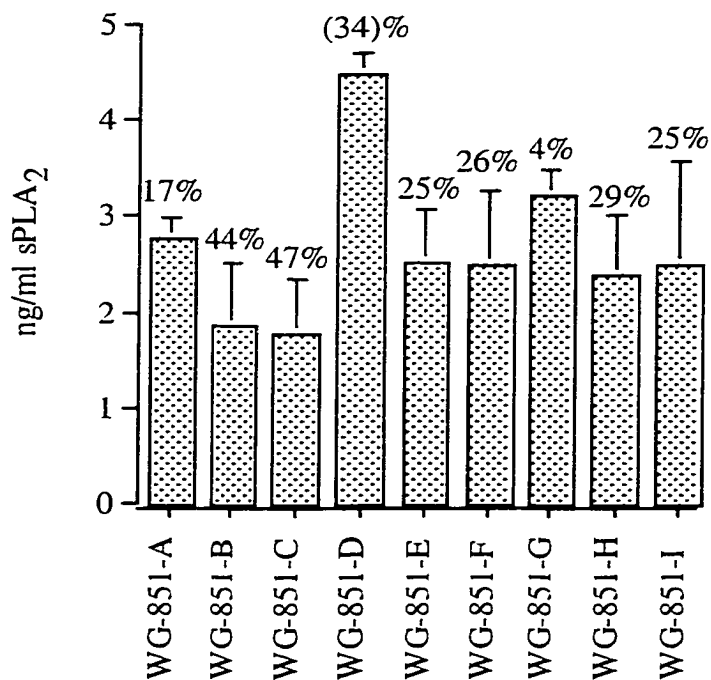


Figure 12. Comparison of the biological activity from the first round of fractionation in the HepG2 model of inflammation. Error expressed as one standard deviation, Numbers represent % inhibition, parentheses > 100% stimulation, N=6.

WG-854 Primary Fractions

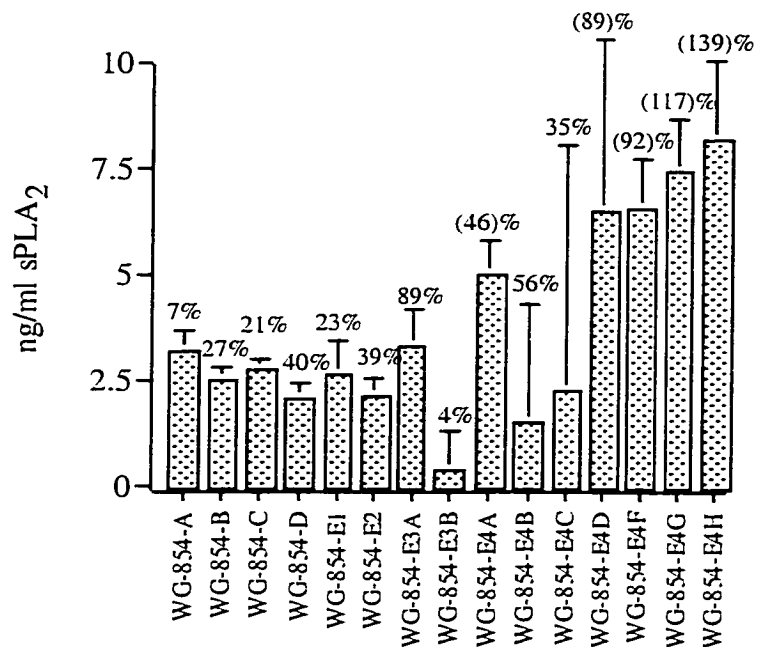


Figure 13. Comparison of the biological activity from the first round of fractionation in the HepG2 model of inflammation. Error expressed as standard deviation, Numbers represent % inhibition, parentheses > 100% stimulation, N=6.

WG-933 Primary Fractions

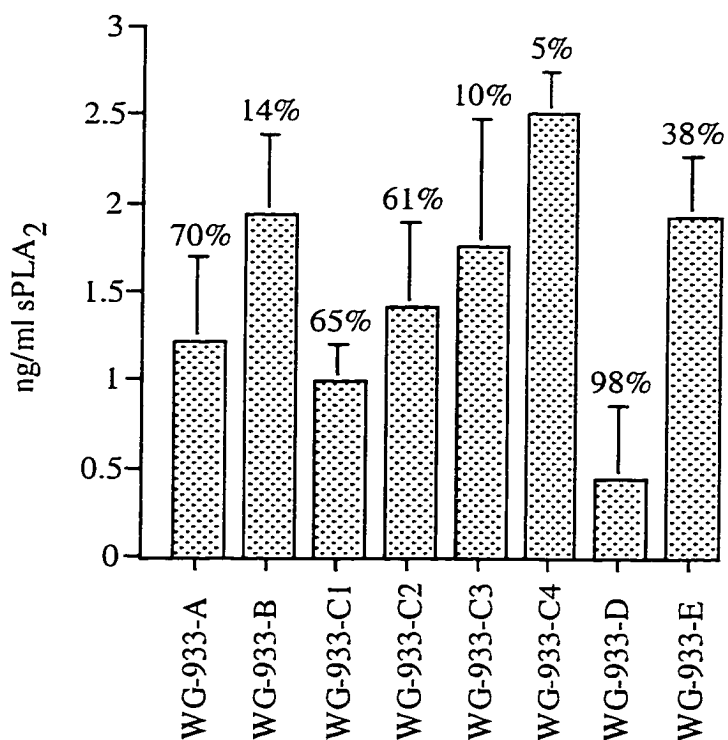


Figure 14. Comparison of the biological activity from the first round of fractionation in the HepG2 model of inflammation. Error expressed as standard deviation, Numbers represent % inhibition, parentheses > 100% stimulation, N=6.

WG-947 Primary Fractions

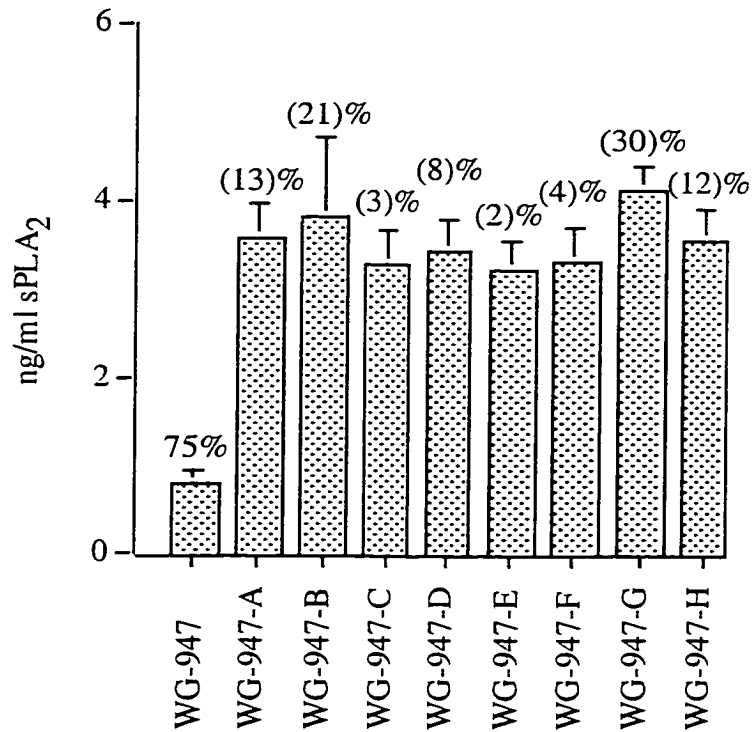


Figure 15. Comparison of the biological activity from the first round of fractionation in the HepG2 model of inflammation. Error expressed as standard deviation, Numbers represent % inhibition, parentheses > 100% stimulation, N=6.

WG-956 Primary Fractions

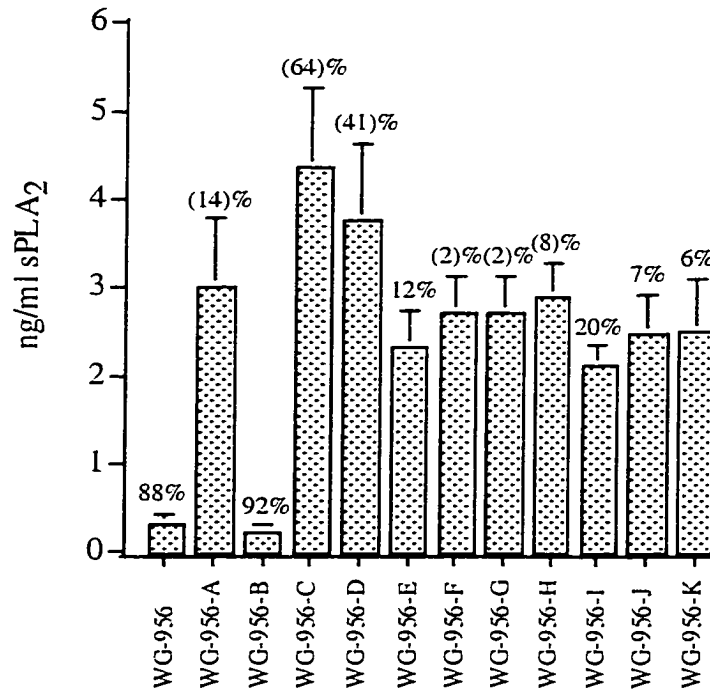


Figure 16. Comparison of the biological activity from the first round of fractionation in the HepG2 model of inflammation. Error expressed as standard deviation, Numbers represent % inhibition, parentheses > 100% stimulation, N=6.

WG-975 Primary Fractions

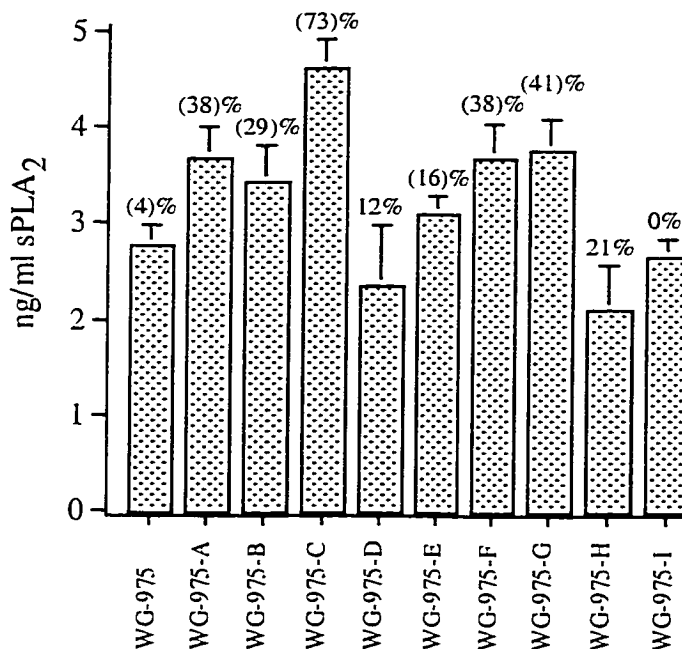


Figure 17. Comparison of the biological activity from the first round of fractionation in the HepG2 model of inflammation. Error expressed as standard deviation, Numbers represent % inhibition, parentheses > 100% stimulation, N=6.

As fractionation proceeded, only these few candidate extracts were carried forward to the next tier of study. In some cases, subfractionation was carried out to the sixth tier (as in the case of WG-933, Figure 18). This led to increasing potency in some

cases(Figure 9-Figure 13 and Figure 15) and complete loss of activity in others (Figure 14 and Figure 16).

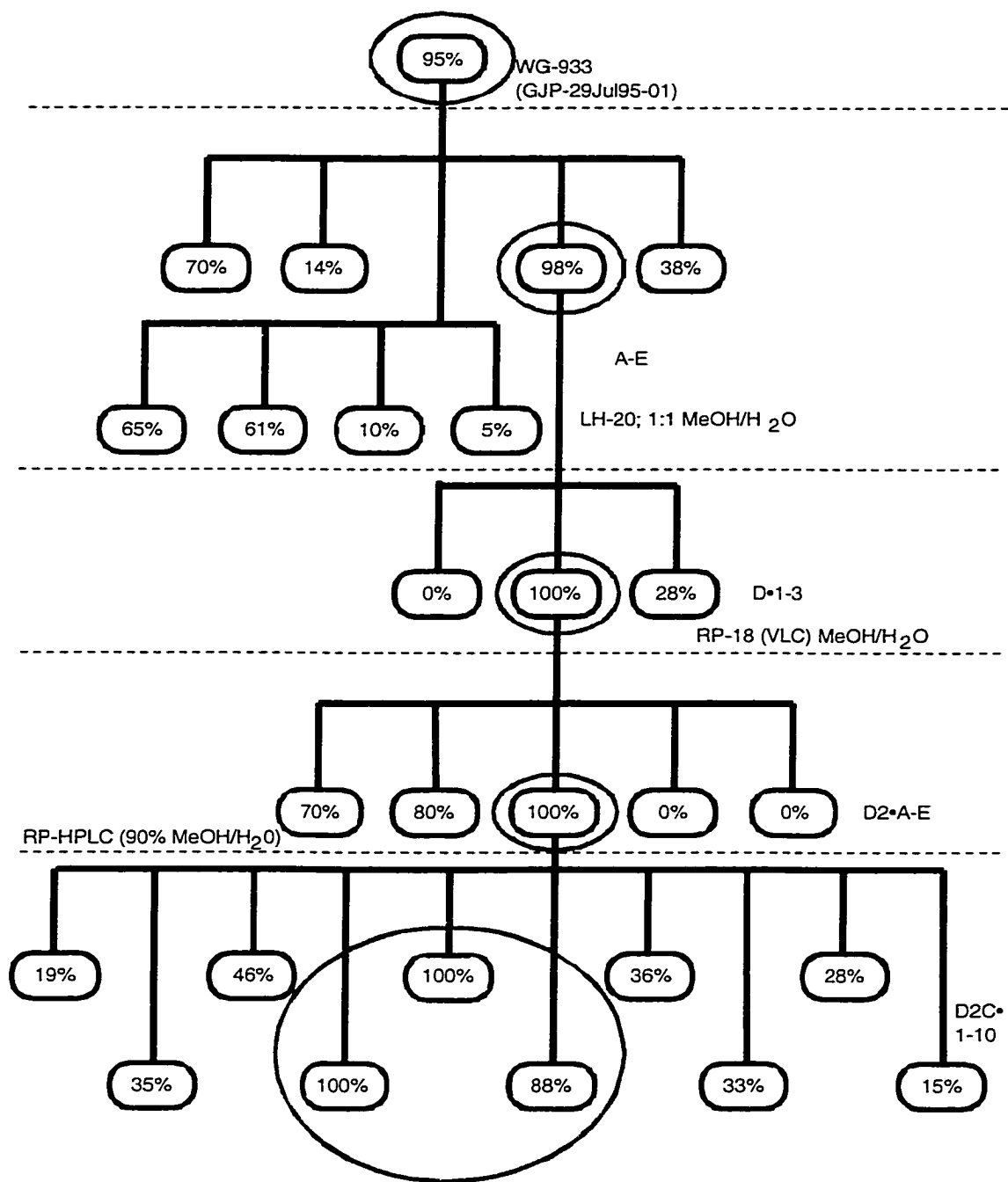


Figure 18. Purification tree for WG-933. Percent inhibition of sPLA₂ in the HepG2 model of inflammation expressed for each extract. Red bubbles represent extracts taken to the next tier of purification, N=6.

For WG-933, the purified compounds and co-purified substances were then tested individually in the model to establish the active compound.

The co-purified malyngamides (example in Figure 19) were not active in this model (Figure 20).

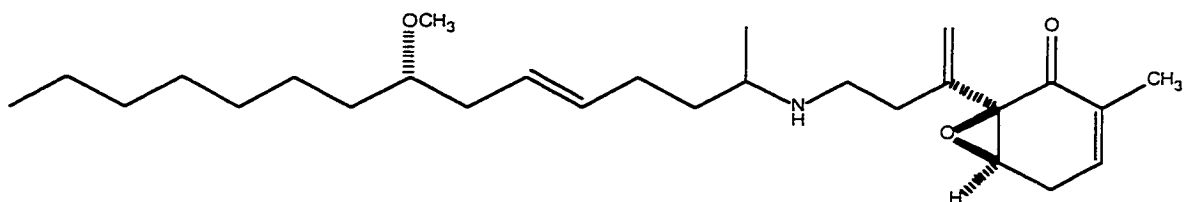


Figure 19. Malyngamide H.

Effect of various Malangamides on HepG2 sPLA₂ secretion.

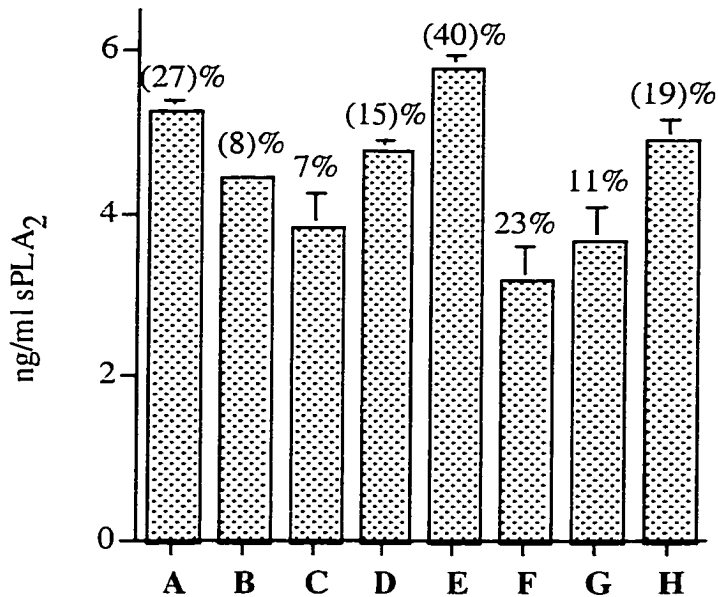


Figure 20. Several Malangamides were tested at 1 μ g/ml in the HepG2 model of inflammation. (**A**: Malyngamide C, **B**: Malyngamide C-acetate, **C**: Malyngamide F-acetate, **D**: Malyngamide H, **E**: Malyngamide I, **F**: Malyngamide J, **G**: Malyngamide L, **H**: Malyngolide) Error expressed as one standard deviation, Numbers represent %, inhibition, parentheses > 100% stimulation, N=6.

Methylation adducts (by-products in the structural elucidation of marine natural products for this work) were also tested and found to be inactive in the model (Figure 21).

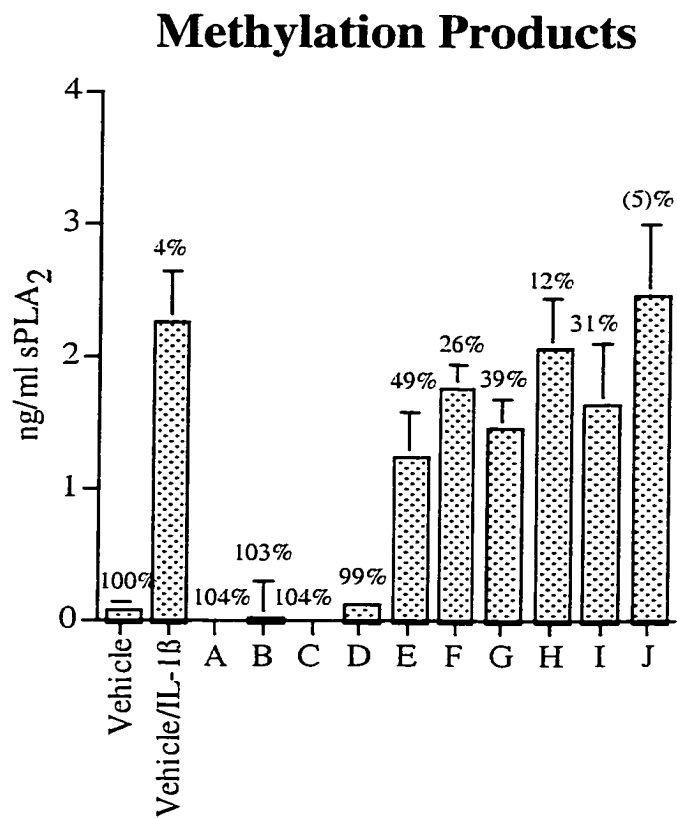


Figure 21. Comparison of the biological activity of methylation products formed in the GC/MS analysis of WG-933D2B,C in the HepG2 model of inflammation. (A: WG-933-D2B 10µg/ml, B: WG-933-D2B 1µg/ml, C: WG-933-D2B-O-Me 10µg/ml, D: WG-933-D2B-O-Me 1µg/ml, E: Ethyl-*p*-toluene Sulfonate 10µg/ml, F: Ethyl-*p*-toluene Sulfonate 1µg/ml, G: (-)-*Trans*-7(S)-methoxytetradec-4-enoic acid 10µg/ml, H: (-)-*Trans*-7(S)-methoxytetradec-4-enoic acid 1µg/ml, I: (-)-*Trans*-7(S)-methoxytetradec-4-enoic-O-Me 10µg/ml, J: (-)-*Trans*-7(S)-methoxytetradec-4-enoic-O-Me 1µg/ml) Error expressed as one standard deviation, Numbers represent % inhibition, parentheses > 100% stimulation, N=6.

The conclusion, therefore, was that the active component contained in the WG-933-D2C5 fraction was possibly the previously described kalkitoxin molecule.

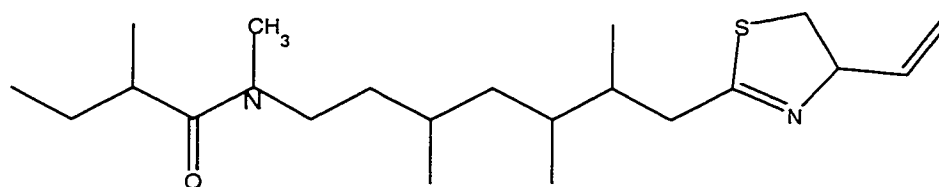


Figure 22. Kalkitoxin

As a serendipitous observation, the model was susceptible to the microtubule destabilizing (MTD) molecule Curacin A, a compound found in WG-956.

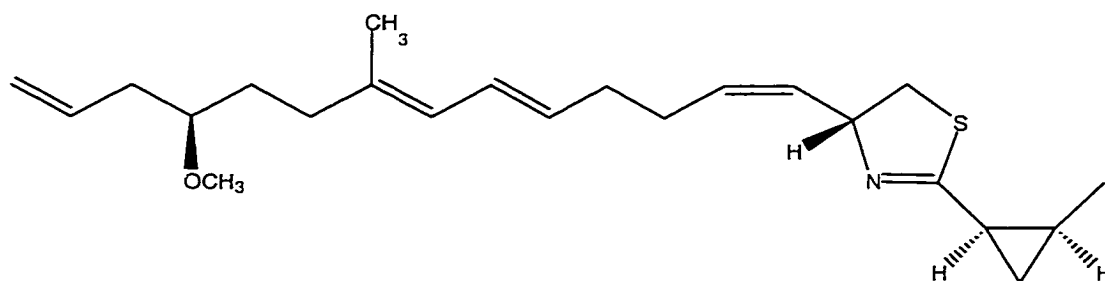


Figure 23. Curacin A

The ability of MTD's to affect the expression of sPLA₂ in other cells has been observed by Pruzanski *et al.* [1995]. This inhibition of sPLA₂ expression was seen with the MTD's vinblastine and Curacin, as shown in Figure 24 below.

Effect of the MTD's Curacin A and Vinblastine on HepG2 sPLA₂

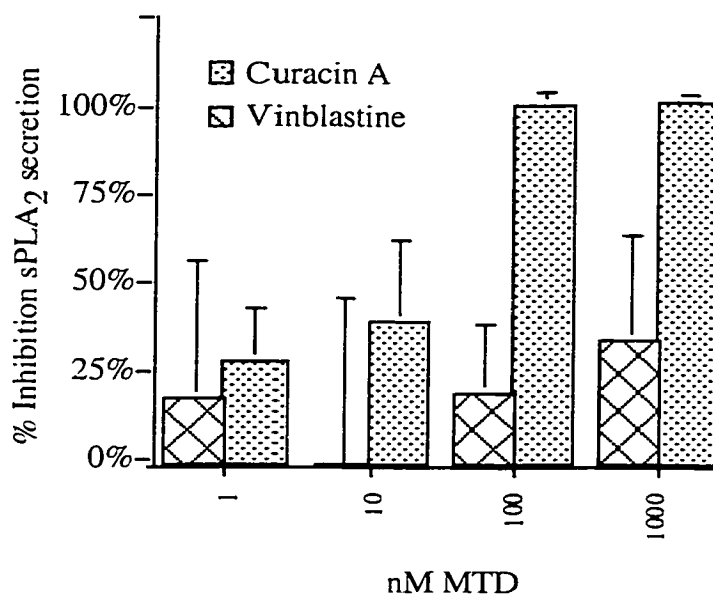


Figure 24. The effect of the Microtubule Destabilizing Compounds (MTD) Curacin A and Vinblastine in HepG2 sPLA₂. Error bars represent one standard deviation, N=6.

3.3 Pharmacological Studies

3.3.1 Kalkitoxin

Kalkitoxin has been previously investigated by researchers at Oregon State University, College of Pharmacy (unpublished data) where fractions of *Lyngbya majuscula* have yielded this compound. Kalkitoxin has ichthyotoxic ($LC_{50} = 5 \text{ ng/ml}$, goldfish) and invertibraticidal activities ($LC_{50} = 28 \text{ ng/ml}$ in the brine shrimp *Artemia salina*, and $28 \mu\text{g/ml}$ and in the freshwater pulmonate snail *Biomphalaria glabrata*). In the HepG2 assay, kalkitoxin was identified in active fractions via bioassay-guided fractionation ($ED_{50} = 7 \text{ nM}$) from WG-933. The active extracts contained the previously characterized kalkitoxin molecule. This cyanobacterium (*Lyngbya majuscula*) has been shown to produce the Malyngamides, a related class of isoprenoids [Cardellina 1978].

To determine whether kalkitoxin was acting like a MTD, the sea urchin embryo assay was used. The effect of kalkitoxin on fertilized embryos is shown in Figure 25.

Effect of WG-933 D2C5 on sea urchin embryo division.

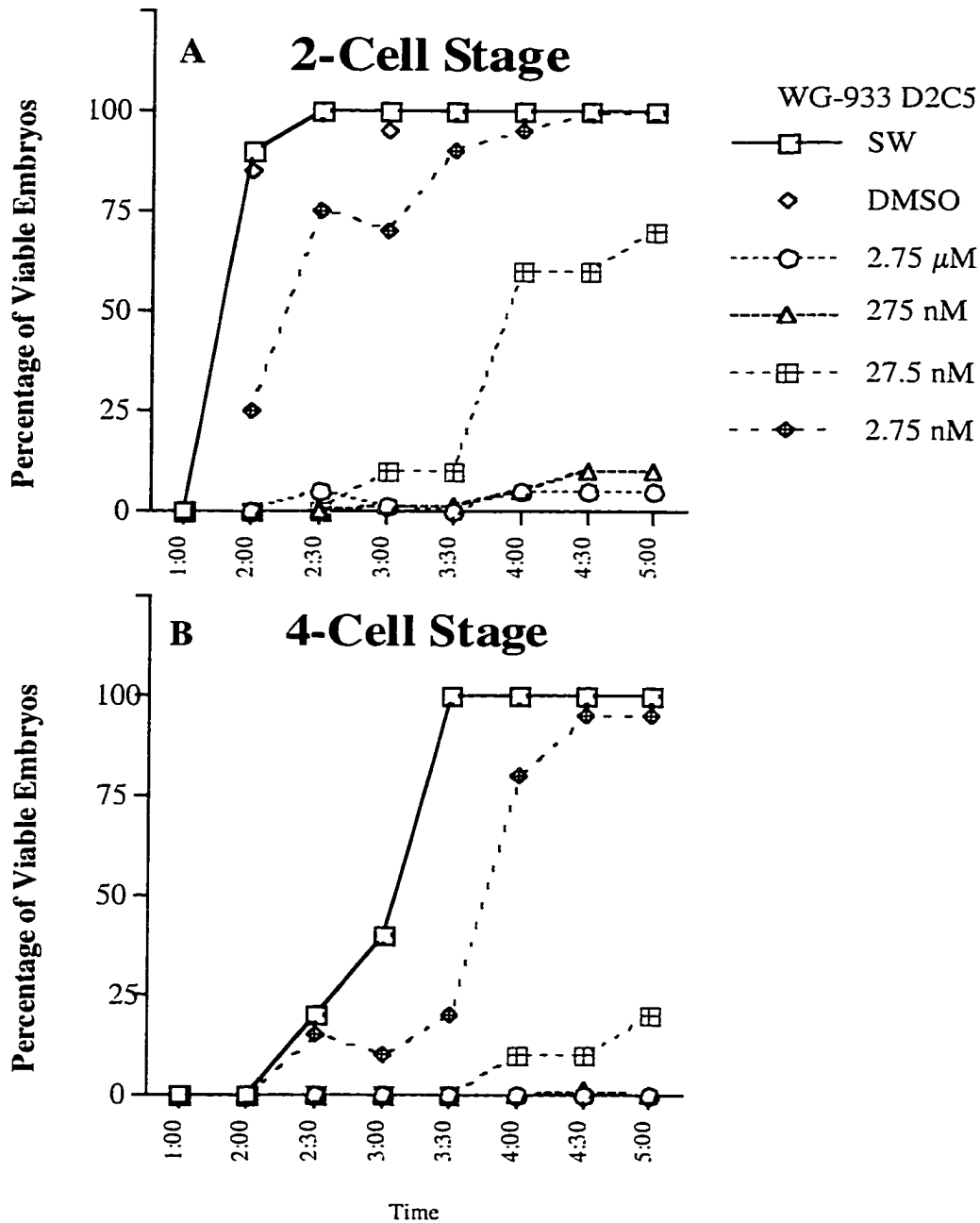


Figure 25. The effect of the active fraction from the HepG2 model of inflammation on the rate of fertilized sea urchin embryos reaching the 2-celled (A) and 4-celled (B) stages of division, $N \geq 200$.

The ED_{50} for inhibition of urchin embryo division was approximately 10 nM. The relationship between the effective doses in the HepG2 model and the effect on urchin embryo division is shown in Figure 26.

Effect of WG-933 D2C5 on sea urchin embryo division and HepG2-sPLA₂ secretion

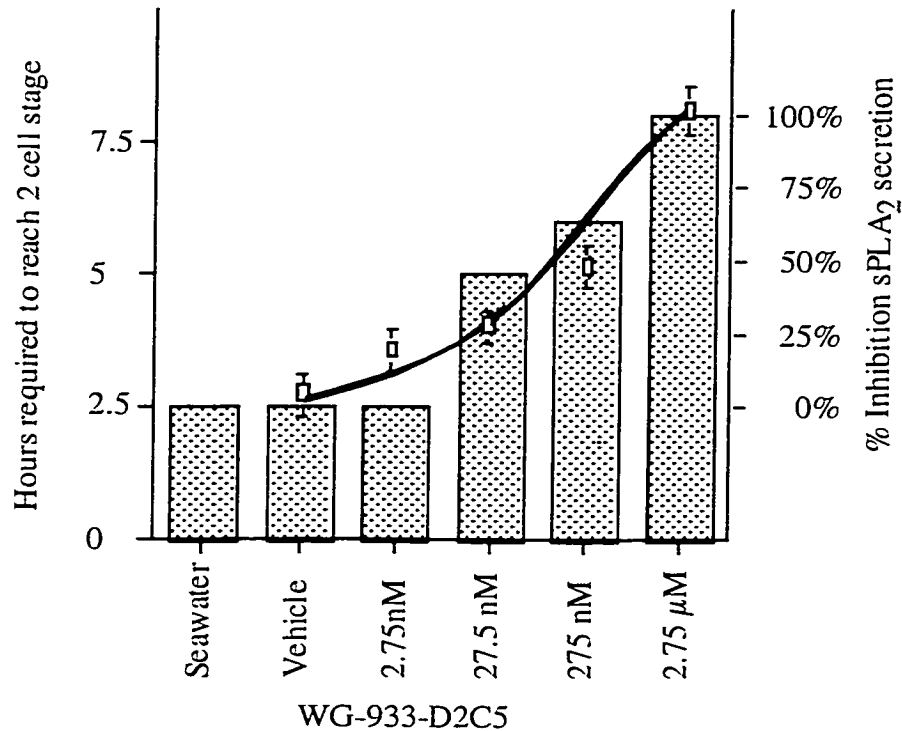


Figure 26. Dose/response of HepG2 cells to WG-933 D2C5. The bars represent the number of hours required to pass greater than 90% of viable embryos through the first division ($N \geq 200$). The curve and boxes with standard error expressed as standard deviation, represent the dose/response of HepG2 cells to WG-933 D2C5, $N=6$.

Additionally, several attempts were made to test kalkitoxin on purified microtubules. By microscopic examination, there was no significant difference between control and kalkitoxin-treated microtubules. After repeating the HepG2-sPLA2 study on the kalkitoxin sample, it appears that anti-inflammatory activity had been lost from these same samples (35% reduction in inhibitory activity). This suggests that the sample may have degraded before the purified microtubule study had been performed. No further sample was available to test in the model.

3.3.2 Ceratospongamides

Ceratospongamides (WG-854) were isolated from a symbiosis consisting of a marine sponge (*Ceratodictyon spongiosum*) and red macroalga (*Sigmatocia symbiotica*). After isolation, two stable conformers were purified. Each consisted of two L-phenylalanine residues, one (L-isoleucine)-L-methyl-oxazoline residue, one L-proline residue and one (L-proline)-thiazole

residue. The major fraction (80%) was *cis-cis* with respect to amide linkage of the prolines.

This Page Intentionally Left Blank

B *trans-trans* Ceratospongamide

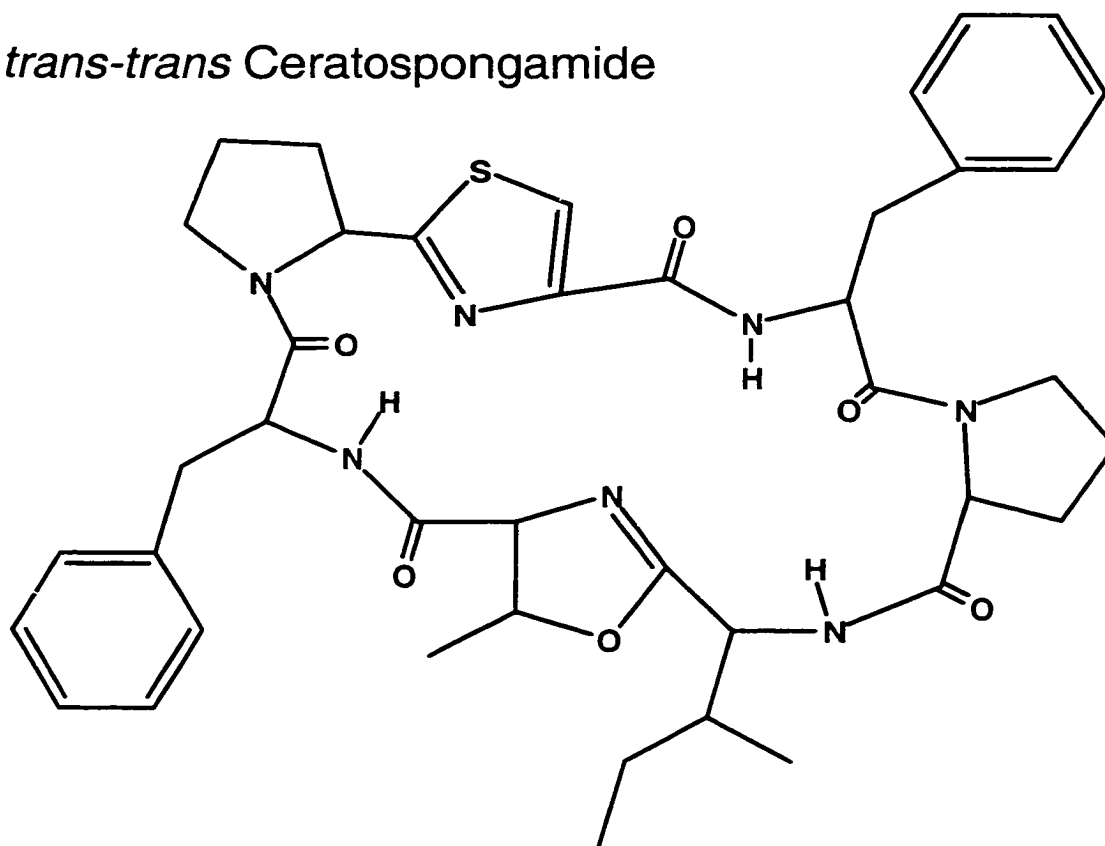


Figure 27. Ceratospongamides A and B.

The *Trans-trans* ceratospongamide conformer, unlike *cis-cis* ceratospongamide, was found to be very potent in the HepG2 model ($ED_{50} = 32$ nM, Figure 28).

Dose-Response for *trans-trans* Ceratospongamide in the HepG2 model of inflammation.

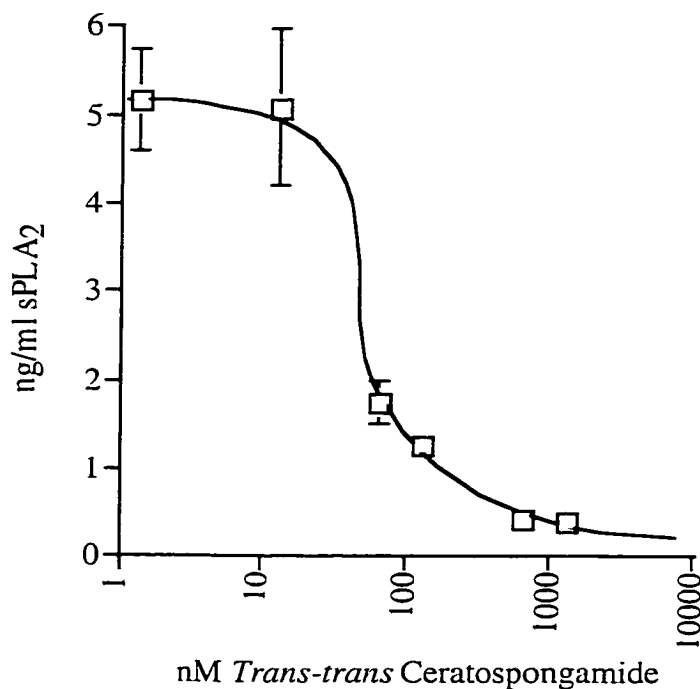


Figure 28. Log-dose/response relationship for *trans-trans* ceratospongamide in the HepG2 model. Error bars represent one standard deviation, N=6.

The structure of ceratospongamide was deduced to be a cyclic peptide, and therefore, it was postulated that other cyclic peptides would behave like the active ceratospongamide. To test the susceptibility of the HepG2 cells to other cyclic peptides,

several similar peptide sequences were tested in the model. Peptides 1 through 4 are (L-proline)-methyl-thiazole, (L-isoleucine)-oxazoline, L-phenylalanine; (L-proline)-methyl-thiazole, (L-isoleucine)-oxazoline, L-phenylalanine, (L-isoleucine)-oxazoline; (L-proline)-methyl-thiazole, (L-alanine)-oxazoline, L-phenylalanine; and (L-isoleucine)-methyl-oxazoline, (L-phenylalanine)-thiazole, (L-isoleucine)-methyl-oxazoline, (L-alanine)-thiazole respectively. The activities of these compounds are listed in Table 7:

Molecule	% Inhibition
Peptide 1	-35±20%
Peptide 2	-15±12%
Peptide 3	12±7%
Peptide 4	-21±24%

Table 7. The cyclic peptides above were tested under identical conditions to *trans-trans* ceratospongamide. Negative numbers represent greater than control stimulation ± one standard deviation, N=6.

To test the ability of *trans-trans* ceratospongamide to inhibit microtubule stability, the sea urchin embryo assay was used. The

effects of *trans-trans* ceratospongamide on fertilized sea urchin embryos are shown in Figure 29.

***Trans-trans* Ceratospongamide effects on urchin embryo division rate.**

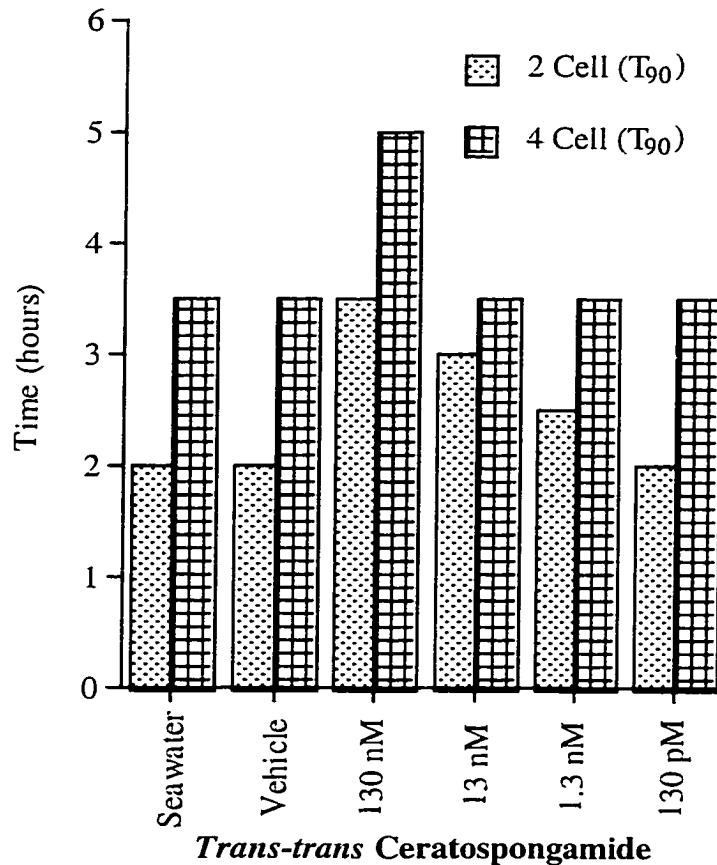




Figure 29. Bars represent the time required (hours) for at least 90% of viable embryos to reach the first () or second () cell division. Vehicle is DMSO 0.1%. Less than 0.5% cytotoxicity for all treatments, 97% fertilization efficiency, *Strongylocentrotus purpuratus*, N>300.

Like kalkitoxin, there is an effect of *trans-trans* ceratospongamide on the rate of embryo division at the IC₅₀ for sPLA₂ secretion in the HepG2 model of inflammation (Figure 30). The relationship between the dose and its effect on sPLA₂ expression and inhibition of embryo division is similar, but this effect does not persist into the 4-cell stage with ceratospongamide

Effect of *trans-trans* Ceratospongamide on urchin embryo division and HepG2-sPLA2 secretion

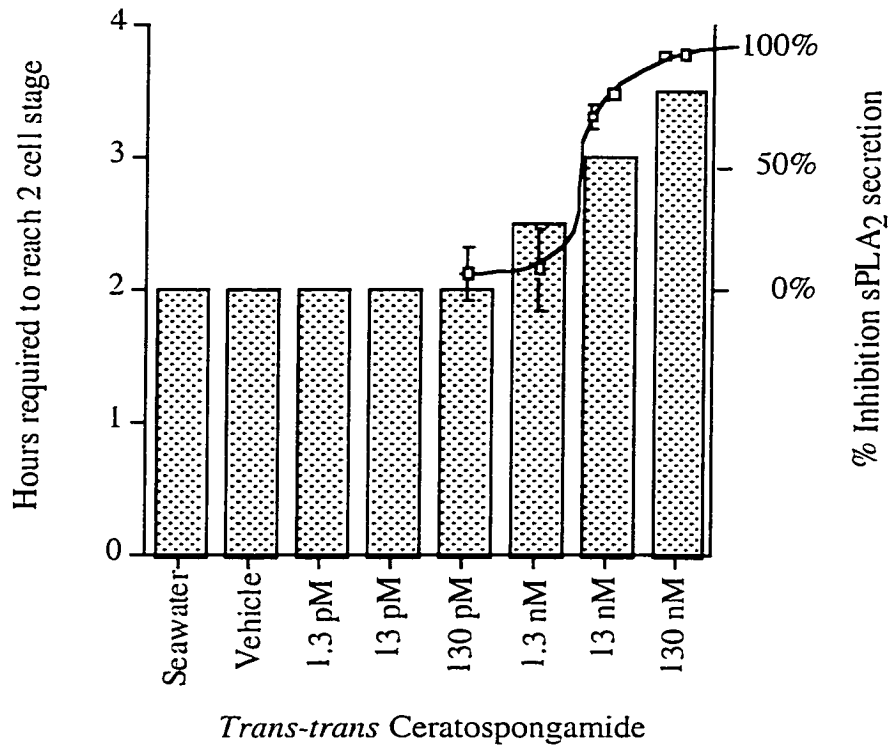


Figure 30. The left y-axis and bars represent the number of hours required to pass greater than 90% of viable embryos through the first division ($N > 200$). The right y-axis and line represent the dose/response of HepG2 cells to *trans-trans* Ceratospongamide. Error expressed as standard deviation, ($N=6$).

However, as can be seen in Figure 29, this effect disappears for all but the highest concentration at the four-cell stage.

The HepG2 model was used for both the second and third phase of this project. The second phase having been completed, the cells were now used for reporter assays. The reporter allows a specific, truncated portion of the promoter of a gene to be studied. By using two strongly promoted reporters (reporters which have a detectable level of basal expression), it was possible to study inhibitory effects of compounds that were active in the screening model. A second advantage of this application of these molecular tools was the ability to simultaneously collect conditioned media and to correlate the mass of expressed sPLA₂ with the mass of accumulated reporter gene (chloramphenical acetyl transferase). Further investigation of *trans-trans* ceratospongamide involved the transient transfection of HepG2 cells with CAT reporter constructs based upon the sPLA₂ promoter. In IL-1 β stimulated (400 pg/ml), reporter-transfected HepG2 cells pretreated with *trans-trans* ceratospongamide (50

ng/ml), the expression of the reporter (-326 to +20) was reduced by 50% relative to control and 90% in the (-159 to +20) plasmid construct. This indicated a potentially significant role for the transcription factor site located in this region.

Electrophoretic mobility shifts were performed with IL-1 β and *trans-trans* ceratospongamide to test the activated HepG2 cells for the ability to bind the AP-1 consensus sequence (a sequence located in the human sPLA₂ promoter at -119, as shown below.

-327

GAGGCGATTG CAGGGAGGTG GCTGACCGTT GATCACACCC
AGAGGCTGGT TATGGGAATT TACTCCATGG AAAGACTCGG
CAAAC|TGCC TGAAT|GTG|TT T|GGCAT|CAG| GCTACTGACA
CGTAAGGG|TT TCCCAAT|CCT CAACTCTGTC CTGGCCAGGC
TGATGAGGGG AAGGAAAGGG ATTACCTAGG GGTATGGGGC
ACCA|ATCC|TG AGTCCA|CAA CTGA|CCACGC CCATC|CCCAG
CC|TTGTGCCT CACCTACCCC CAACCTCCAG AGGGAGCAGC
TATA
|ATTTA|AGGG GAGCAGGAGT GCAGAACAAA CAAGACGGCC
TGGGGATACA ACTCTGGAGT CCTCTGAGAG
+23

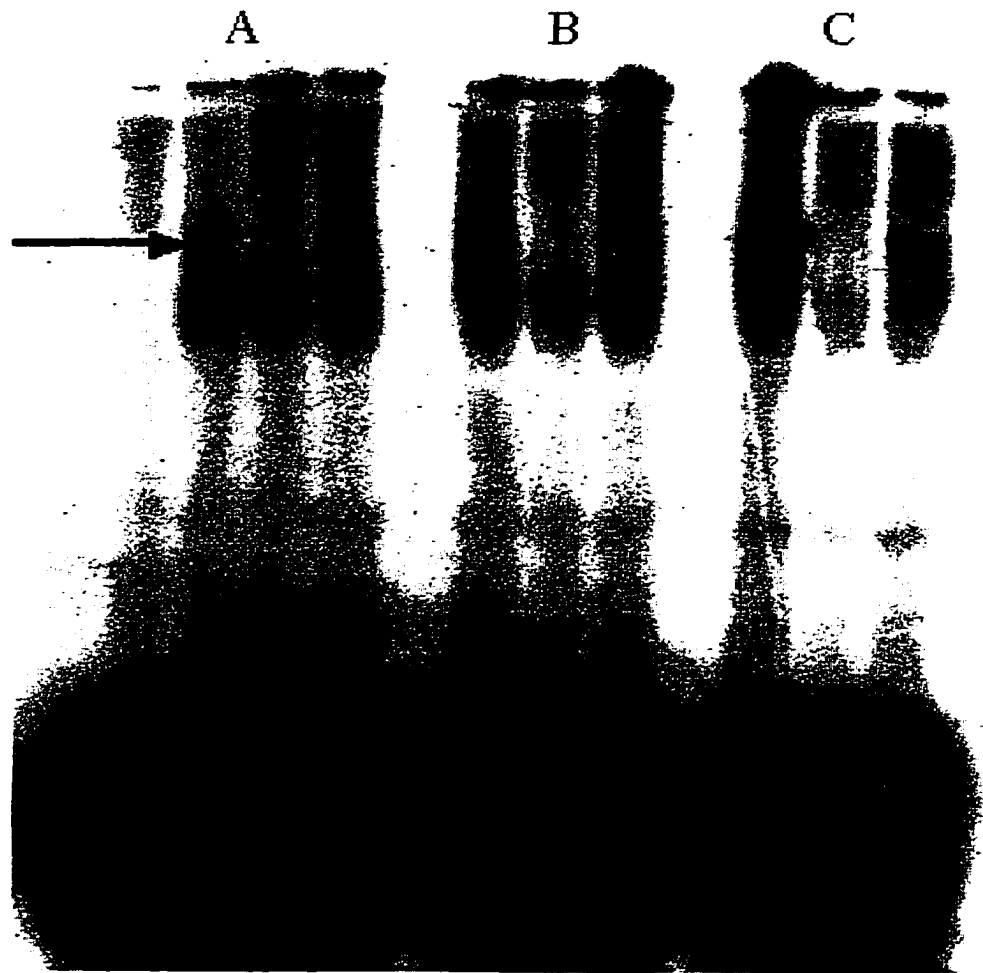
Element A	TATA-Box Containing Sequences
Element B	Positive Regulatory Elements
Element C	Negative Regulatory Elements
Element D	Negative Regulatory Elements

Olivier *et al.* 1994

Figure 31. The proximal portion of the sPLA2 promoter. The IL-6 regulated elements A-D are color coded pink, green, light and dark blue respectively. Interleukin-sensitive elements are marked in the sequence by bars.

In IL-1 β stimulated, reporter-transfected HepG2 cells pretreated with *trans-trans*-Ceratospongamide (50 ng/ml), the expression of the reporter (-326 to +20) was reduced by 50% relative to control and 90% in the (-159 to +20) plasmid construct.

The gel shifts with the AP-1 consensus oligonucleotide (sequence) are shown in Figure 32.



Unlabelled Probe	-	-	+	-	-	+	-	-	+	-
Nonspecific Competitor	-	-	-	+	-	-	+	-	-	+

Figure 32. Electrophoretic Mobility Shift Assay for AP-1 consensus sequence binding. Control (A), IL-1 β stimulated (B) and *trans-trans* Ceratospongamide pretreated, IL-1 β stimulated (C) HepG2 nuclear extracts were tested. Lane A.1 lacks nuclear extracts as a background control. The arrow marks the point of migration for the AP-1 / 32P-Probe complex in the gel.

Control levels of AP-1 binding are low, and specific (as shown by competition with unlabeled AP-1). In the presence of IL-1 β , this specific binding increases dramatically. After pre-incubation with *trans-trans* ceratospongamide (1 μ g/ml, 1 hour), IL-1 β causes an accumulation of proteins capable of binding AP-1 consensus in the nucleus of the HepG2 cells. The presence of *trans-trans* ceratospongamide alters the specificity of the nuclear extract to nonspecific oligonucleotide (OCT-1). OCT-1 does not appear in the human sPLA₂ promoter. This seems to indicate some role of ceratospongamide in nuclear signaling by altering the specificity of transcription factor binding. The consensus sequences are shown in Table 8.

AP-1 5'-cgc ttg atg agt cag ccg gaa-3'
OCT-1 5'-tgt cga atg caa atc act aga-3'

Table 8. Consensus oligonucleotides used in the AP-1
Electrophoretic Mobility Shift assay.

As can be seen in Figure 32, where *trans-trans* Ceratospongamide is used (lanes C.1 through C.3), there is a marked decrease in the binding of nuclear factors to the AP-1 consensus in the presence of both unlabeled specific probe (C.2) and the unlabeled non-specific probe OCT-1 (C.3). This result is inconclusive and deserves further study.

4 Conclusions

4.1 Model Development

This project involved a multiple-phase exploration of cellular and molecular models of inflammation. The target disease was primarily arthritis. To model the disease milieu in culture, rheumatoid fibroblasts were isolated, cultured and studied. Furthermore, it was determined that the level of desired pharmacological intervention was targeted at the expression of an important inflammatory mediator. Therefore, the first phase of exploration involved an evaluation of rheumatoid synovial fibroblasts for secreted factors. sPLA₂ was ultimately chosen because of its relevance and ease of study. This choice was based upon preliminary work in this area.

4.2 Target Selection

Secreted PLA₂ is a clinically relevant marker of both rheumatoid arthritis and sepsis [Olivier 1994, Crowl 1991, Mochan 1989]. I hoped that a molecule could be found that had a therapeutic

application in the treatment of rheumatoid arthritis. To this end, several cell lines were used in the development of the model of rheumatoid disease. This choice was necessary because of the inherent variability of the human sources previously used for the fibroblast work. Previous studies of sPLA₂ had been carried out in many cell types, but very significant regulatory work had been completed in the HepG2 cell line [Olivier 1994, Crowl 1991]. The HepG2 cell provides a human cell type and the origin of these cells, the liver also provides a relevant target for sepsis study. Sepsis may be a secondary target for the compounds discovered through this work. Previously, the HepG2 cell line was used for transfection studies [Olivier 1994], Olivier *et al.* Have shown that the HepG2 cells provide an easily obtained cellular system for transient transfection, allowing an easily obtained molecular target in the form a reporter construct.

4.3 Model Profiling

The microtubule destabilizing compounds (MTD) have the ability to attenuate sPLA₂ secretion in several cell types [Pruzanski

1997]. This is a direct effect of the transport mechanism used to transduce the IL-1 β signal to the nucleus of the cell. The urchin embryo assay is also sensitive to MTD's, displaying the destabilizing activity in a retarded or inhibited division of fertilized embryos. To confirm the importance of microtubule poisons in the HepG2 model, two MTD's were used. Vinblastine, an MTD, showed some activity in this model. Secondly, a metabolite from *Lyngbya majuscula*, Curacin A, was tested (Figure 24). This molecule has a potent activity in the sea urchin embryo assay. Additionally, Curacin A was a potent inhibitor of sPLA₂ secretion from IL-1 β stimulated HepG2 cells. This compound was purified from the bank of marine natural produces where it is designated WG-956.

Other anti-inflammatory compounds were tested in the model to determine the potential susceptibility of the IL-1 β signaling pathway in HepG2 cells. Among these compounds (Table 5) were the I κ B-Kinase inhibitors BAY 11-7082 and 85. These compounds have the potential for inhibiting NF κ B-induced expression of

protein, by affecting the NFkB signaling pathway. These compounds showed a high degree of cytotoxicity (35-40%, LDH). Dexamethasone, an anti-rheumatic steroid, showed some effect (66%), confirming that this model might be useful in detecting new steroidal compounds. Negative controls (LO and Co inhibitors) showed a low level of sPLA2 production inhibition.

De novo synthesis of IL-1B-induced sPLA2 production in HepG2 cells was confirmed by Cycloheximide inhibition.

4.4 Pharmacological Studies of *Ceratodictyon spongiosum* extracts.

From extracts of *Ceratodictyon spongiosum*, compounds had been purified to homogeneity and their stereochemistry determined in two rounds of purification. The active compound is a fraction of a pair of co-purified conformers. The minor fraction, *trans-trans* ceratospongamide, is very potent (fig. 23, ED₅₀ 32 nM), while the *cis-cis* ceratospongamide is inactive at 32 μM. This activity was determined by sPLA₂ ELISA. This pair of conformers offers an

interesting area for investigation. As can be seen in Figure 27, there is some flexibility in the backbone of these compounds, which permits these two molecules to assume dramatically different 3-dimensional conformations. Under biological conditions, there is no activity in the *cis-cis* conformer (at 1000 times the ED₅₀ of the active conformer).

4.4.1 Sea Urchin Assay

Further investigation of the compound showed little effect on microtubule polymerization in the sea urchin fertilization assay. This assay has been used previously to study microtubule destabilizing compounds [Pruzanski 1997]. The urchin assay is sensitive to vinblastine, colchicine, and Curacin A. The active *trans-trans* conformer was found to have almost no detectable effect on the rate of embryo division in the urchin assay at the four-cell stage and only a weak effect at two-cell stage of cell division (Figure 29). As can be seen in Figure 30, there is an order of magnitude difference in the potency of *trans-trans*

ceratospongamide in HepG2 cells and urchin embryos, in contrast to data presented on kalkitoxin, which apparently has MTD activity. Therefore, it is believed that this compound is not acting directly on the transport of the IL-1 β signal from the cell surface.

4.4.2 CAT Reporter Assay

Reporter constructs containing the promoter region of the sPLA₂ gene were available as tools to explore a potential site of action of *trans-trans* ceratospongamide: the promoter region of the type sPLA₂ gene. The sequence of the sPLA₂ gene has been analyzed and some of its transcription factor sites have been mapped [Figure 31, Kramer 1989, Olivier 1994]. Various length promoter sequences ligated to the CAT reporter have been used to describe putative positive and negative regulatory elements in the IL-6 induced expression of the sPLA₂ gene in sepsis by Olivier *et al.* Olivier *et al.* have focused on the role of the upstream regulatory elements apparently responsible for repressing the expression of sPLA₂ with acute stimulation [Qishi 1997] by cytokines. Although

the models developed here rely upon IL-1 β induction, the promoter remains the same, allowing the use of the constructs to determine potential sites of action for the *trans-trans* ceratospongamide in the IL-1 β signaling pathway. Ultimately, the dramatic reduction of CAT expression hinted at some effect of *trans-trans* ceratospongamide on signal transduction or protein expression. To test this hypothesis, EMSA's were performed on known, putative pharmacophores, for the cyclic peptide.

4.4.3 Electrophoretic Mobility Shift Assay

After the reporter studies, expression of the sPLA₂ by HepG2 cells were apparently sensitive to *trans-trans* ceratospongamide. The reporters used were based on the proximal portion of the sPLA₂ initiation site. The AP-1 consensus (an IL-1 β responsive element) located at -119 was tested with nuclear extracts from *trans-trans* ceratospongamide-treated HepG2 cells. Unfortunately, although the nuclear extracts bound specifically to the consensus, there was little apparent effect on the specific binding of the extracts to

the sequence. Thus, there was no direct effect on the binding of AP-1 to the promoter of sPLA₂. However, there was an alteration of the binding specificity of the nuclear extract, suggesting a potential non-specific effect on transcription factor binding. This could account for the observed results in the reporter assay and the cellular model because reduced binding of AP-1 will lead to reduction of CAT and sPLA₂ expression.

4.5 Pharmacological Studies of Lyngbya majuscula

The second candidate compound has been identified as kalkitoxin. This compound was previously identified by Min Wu (personal communication). With the additional data presented here, a putative effect of kalkitoxin has been formulated. Unlike the previously described ceratospongamide, the kalkitoxin isolation required six stages of extract fractionation (Figure 18). During the second stage of study, several extracts from the same species (from different localities) were included. One of these contained Curacin A. This compound appeared in bioassay-guided purification as a strong inhibitor of sPLA₂ secretion. This

observation played an important role in determining how to discern the activity of kalkitoxin. Through the series of purification and chemical analysis steps, several methylation adducts and by-products were tested for activity because of their presence in the purification tree. None of these byproducts showed any significant activity. Kalkitoxin was eventually resolved from the active fractions. However, like Curacin A, this compound is unstable.

4.5.1 Microtubule Studies

The previously described microtubule destabilizing activity was then investigated in both sea urchin embryo and purified microtubule assays. There was a strong MTD effect caused by the kalkitoxin in the sea urchin assay. This effect was not reproducible in the purified microtubule assay. As a check of compound lability, the HepG2 assay was performed with the remaining sample. Anti-inflammatory activity was also lost from this sample Therefore suggesting that the compound may have

decomposed, leading to this loss of activity in the final experiments. The compound showed no cytotoxicity in the embryos (as determined by morphological change). The purified extracts also lacked significant cytotoxicity as measured by MTT, LDH and dye exclusion in HepG2 cells.

4.6 Future Work

Although the detailed pharmacological properties of the two compounds were not determined, the nature of their action in the HepG2 model has been explained. Kalkitoxin appears to affect the transduction of the IL-1 β signal to the nucleus via a microtubule-dependant mechanism. *Trans-trans* Ceratospongamide appears to act in the IL-1 β signaling pathway. In the future, as more of these compounds become available, it should be possible to confirm these observations and find the specific sites of action. Furthermore, because of the low cytotoxicity seen in both of these compounds, each may have a potential therapeutic use. The most important assays to be

completed in the future may include the following molecular and biochemical studies.

4.6.1 Structural Analogs.

One of the problems encountered with kalkitoxin was its instability. This problem could be circumvented by construction of stable analogs. The chemical synthesis of this compound would be difficult because of its 6 chiral centers. If a small group of congeners could be isolated from *Lyngbya* sp., it may be possible to complete an intriguing quantitative structure-activity relationship (QSAR) measurement. However, until the susceptibility of the ring in kalkitoxin to oxidation can be reduced, such studies may prove equally daunting.

4.6.2 Northern Blot analysis.

The implications of the data presented here are that there is some effect on the expression and/or release of sPLA₂ from HepG2 cells after exposure to two structurally and phylogenetically unrelated compounds. With a more thorough investigation of the

quantitative effects of kalkitoxin and *trans-trans* Ceratospongamide on mRNA production in hepatocellular carcinoma cells, it will be possible to assign a role of each compound in the progress of IL-1 β -induced inflammatory pathway.

At present, it appears that kalkitoxin is acting on the microskeletal system of the cells, this effect will be observed in a Northern Blot analysis through a dramatic reduction in specific sPLA₂ mRNA. There should also be a concordant reduction in other IL-1 β responsive element species of mRNA.

Trans-trans ceratospongamide also has a reducing effect on the expression of sPLA₂. Like kalkitoxin, ceratospongamide is expected to reduce the level of sPLA₂ mRNA. It remains unclear where the precise site of action lies for this cyclic peptide, however, mRNA levels will give a key to determining the upstream (signaling) or downstream (expression) site.

4.6.3 Electrophoretic Mobility Shift Assay with increased replicates and Supershift Studies.

For *trans-trans* ceratospongamide, additional gel-shift studies would provide more support of the hypothesis that ceratospongamide has an effect on the transcriptional activation of sPLA₂ in HepG2 cells. With the use of more IL-1 β effectors, including AP-1, NFIL-6, and other members of the acute phase group of transcription factors, it may be possible to further confirm or refute the mechanism of action of this cyclic peptide.

4.6.4 Purified Microtubule Assays

Due to an instability problem encountered with kalkitoxin, the sample became damaged while testing with purified microtubules. This problem can be avoided by completing the studies in an anoxic environment. Additional studies by Berman *et al.* (1999) have shown that kalkitoxin can induce time dependant NMDA receptor-mediated neurotoxicity. The connection between the

NMDA receptor and the apparent activity in the sea urchin and HepG2 cells remains to be made.

4.6.5 Additional *In vitro* studies.

Based upon the results of Northern and Gel shift studies, it may be necessary to attempt more studies. Microtubule assays and pre-incubation of specific transcription factors with ceratospongamides may provide important data about the affinity for and activity in the cytoplasmic and nuclear compartments of the cell. Likewise, studies of the receptor-mediated activation of the cells may lead to some insight into the specific mechanism of each molecule. Finally, there may be a post transcriptional or translational effect for each of these compounds that has been overlooked.

5 Bibliography

Bennion C., S Connolly and N Gensmantel. **1992**. Design and synthesis of some substrate analogue inhibitors of phospholipase A₂ and investigations by NMR and molecular modeling into the binding interactions in the enzyme-inhibitor complex. *J. Med. Chem.* **35**:2939-2951.

Berman FW, WH Gerwick, and TF Murray. Antillatoxin and kalkitoxin, ichthyotoxins from the tropical cyanobacterium *Lyngbya majuscula*, induce distinct temporal patterns of NMDA receptor-mediated neurotoxicity. *Toxicon*. **1999** Nov;37(11):1645-8.

Blake DR, PG Winyard and R Marok. **1994**. The contribution of hypoxia-reperfusion injury to inflammatory synovitis: the influence of reactive oxygen intermediates on the transcriptional control of inflammation. *Annals of the New York Academy of Sciences*. **723**:308-17.

Bradford, M. (**1976**) *Annals of Biochemistry*. **72**:248.

Cardellina, JH, D Dalietos, F Marner, JS Mynderese and RE Moore. **1978.** (-)-*Trans-7(S)*-Methoxytetradec-4-enoic acid and related amides from the marine cyanophyte *Lyngbya Majuscula*. *Bioch.* **17**:2091-95.

Case, JP, R Lafytis, GK Kumkumian, EF Remmers and RL Wilder. **1990.** Il-1 Regulation of Transin/stromelysin Transcription in Rheumatoid Synovial Fibroblasts Appear to Involve Two Antagonistic Transduction Pathways. An Inhibitory Prostaglandin-Dependant Pathway Mediated by cAMP, and a Stimulatory, PKC-Dependant Pathway. *J. Immunology.* **145(11)**:3755-61.

Caldwell, JR. **1995.** Medical treatment of rheumatoid arthritis. *Journal of the Florida Medical Association.* **82(5)**:343-7.

Chang , JS, SC Gilman and AJ Lewis. **1986.** Interleukin 1 activates Phospholipase A2 in rabbit chondrocytes : a possible signal for IL-1 action. *J. Immunol.* **136**:1283-1287.

Colville-Nash, PR and DL Scott. **1992.** Angiogenesis and Rheumatoid Arthritis: Pathogenic and Therapeutic Implications. *Annals of Rheumatic Diseases.* **51**:919-925.

Crowl, RM, TJ Stoller, RR Conroy and CR Stoner. **1991.** Induction of phospholipase A₂ gene expression in human hepatoma cells by mediators of the acute phase response. *J. Biol. Chem.* **266**:2647-2651.

Cuchacovich, M, A Tchemitchin, H Gatica, R Wurgaft, C Valenzuecarlos and E Comejo. **1987.** Intrarticular Progesterone: effects of the local Treatment for Rheumatoid Arthritis. *J. Rheum.* **15**(4):561-565.

Damon, M, M Rabier, J Loubatiere, F Blotman and A Crastes de Paullet. **1985.** Glucocorticoid receptors in fibroblasts from synovial tissue. Changes during the inflammatory process, Preliminary results. *Agents and Actions.* **17**(5):478-483.

Dayer, Jean-Michel, SM Krane, R Grahm, G Russell and DR Robinson. **1976.** Production of collagenase and prostaglandins

by isolated adherant rheumatoid synovial cells. *Proc. Natl. Acad. Sci. USA* **73(3)**:945-949.

de Carvalho, MS , FX McCormack and CC Leslie. **1993**. The 85-kDa, Aracidonic Acid-Specific Phospholipase A₂ as an Activated Phosphoprotein in Sf9 Cells. *Biochim et Biophys Acta.*, **306(2)**:534-540.

Dennis, EA **1994**. Diversity of Group Types, Regulation and Function of Phospholipase A₂. *J. Biol. Chem.* **269(18)**: 13057-13060.

Dennis EA **1997**. The Growing Phospholipase A₂ superfamily of Signal Transduction enzymes. *Trends in Biochemical Sciences.* **22**:1-2.

Dignam, JD, RM Lebovitz and RG Roeder. **1983**. Accurate transcriptional initiation by RNA polymerase II in a soluble extract from isolated mammalian nuclei. *Nucleic Acids Res.* **11**:1475-1489.

Farrell AJ; Williams RB; Stevens CR; Lawrie AS; Cox NL; **1992**.
Exercise induced release of von Willebrand factor: evidence for
hypoxic reperfusion microvascular injury in rheumatoid arthritis.
Annals of the Rheumatic Diseases. **51(10)**:1117-22.

Flower, RJ and NJ Rothwell. **1994**. Lipocortin-1: Cellular
Mechanisms and Clinical Relevance. *Trends Pharm. Science*.
15:71-76.

Glaser, KB, TS Vedvick and RS Jacobs **1988**. Inactivation of
Phospholipase A₂ by Manoalide: Localization of the Manoalide
Binding Site on Bee Venom Phospholipase A₂. *Biochemical
Pharmacology*. **37(19)**:3639-3646.

Glaser, KB, D Mobilio. JY Chang and N Seko. **1993**.
Phospholipase A₂ enzymes: Regulation and Inhibition. *Trends
Pharm. Science*. **14(3)**:92-8.

Hollenbach, P, D Zilli and S Laster. **1992**. Inhibitors of
Transcription and Translation Act Synergistically with Tuinor

Necrosis Factor to Cause Activation of Phospholipase A₂. *J. Biol. Chem.* **267**(1):39-42.

Hower, RJ and NJ Rothwell. **1994**. I-ipocortin-1: Cellular Mechanisms and Clinical Relevance. *Trends in Pharm. Science.* **15**:71-76.

Hulkower, K, W Hope, T Chen, C Anderson, J Coffey and D Morgan. **1992**. Interleukin-1 β Stimulates Cytosolic PLA₂ in Rheumatoid Synovial Fibroblasts. *BBRC.* **184**(2):712-718.

Jacobson PB; Jacobs RS. **1992**. Fuscocide: an anti-inflammatory marine natural product which selectively inhibits 5-lipoxygenase. Part II: Biochemical studies in the human neutrophil. *Journal of Pharmacology and Experimental Therapeutics.* **262**(2):874-82.

Kramer, RM, C Hession, B Johansen, G Hayes, P McGray, E Pingchang, R Tizard and B Pepinsky. **1989**. Structure and Properties of a Human Non-Pancreatic Phospholipase A₂. *J. Biol. Chem.* **264**:5768-5775.

Kramer R and H Arita. **1994**. Pancreatic Phospholipase A₂ Induces Group II Phospholipase A₂ Expression and Prostaglandin Biosynthesis in Rat Mesangial Cells. *J. Biol. Chem.* **269**(7):5091-5098.

Konieczkowski, M And J Sedor. **1993**. Cell-specific Regulation of Type II Phospholipase A₂ Expression in Rat Mesangial Cells. *J. Clin. Invest.* **92**:2524-2532.

Kunsch, C, and CA Rosen. **1993**. NFκB subunit-specific regulation of the Interleukin-8 promoter. *Mol. Cell. Biol.* **13**:6137-6146.

Laniado-Schwartzman, M, Y Lavrosky, RA Stoltz, MS Connors, JR Falck, K Chauhan and NG Abraham. **1994**. Activation of nuclear factor κB and oncogene expression by 12(R)-hydroxyeicosatrienoic acid, an angiogenic factor in microvessel endothelial cells. *J. Biol. Chem.* **269**:24321-24327.

Leslie, CC. **1991**. Kinetic Properties of a High Molecular Mass Arachidonyl-Hydrolyzing Phospholipase A₂ that Exhibits

Lysophospholipase Activity. *J. Biol. Chem.*, **266**(17):11366-11371.

Marshall LA, JD Winkler, DE Griswold, B Bolognese, A Roshak, CM Sung, EF Webb and R Jacobs. **1994** Effects of scolaradial, a Type II phospholipase A₂ inhibitor, on human neutrophil arachidonic acid mobilization and lipid mediator formation. *JPET*. **268**(2):709-17.

Mayer, R and L Marshall. **1996**. Therapeutic regulation of 14 kDa phospholipase A₂(s). *Exp. Opin. Invest. Drugs*. **5**(5):535-553

Mizel, SB, JM Dayer, SM Krane and SE Mergenhagen. **1981**. *Proc. Natl. Acad. Sci.* 78:2472.

Mochan, E, B Ross, R Sporer and J Uhl. **1989**. Interleukin-1 mediated signal transduction associated with synovial activation. *Agents Actions*. **27**(3/4):282-284.

Morales-Ducret, J, E Wayner, M Elices, J Alvaro-Gracia, N Zvaifler and G Firestein. **1992**. α 4/B1 Integrin (VLA-4) Ligands in

Arthritis: Vascular Cell Adhesion Molecule-1 Expression in Synovium and on Fibroblast-Like Synoviocytes. *Journal of Immunology* **149(4)**:1424-31.

Muhl, H, T Geiger, W Pignat, F Marki, H Van den Bosch, N Cerletti, D Cox, G McMaster, K Vosbeck and J Pfeilschifter. **1992**. Transforming growth factors type-B and dexamethasone attenuate group II phospholipase A₂ genetic expression by Interleukin-1 and forskolin in rat mesangial cells. *FEBS letters*. **310(2)**:190-194.

Mukherjee, A, E Cordella-Mele and L Miele. **1992**. Regulation of Extracellular Phospholipase A₂ Activity- Implication for Inflammatory Disease. *DNA and Cell Bio*. **11(3)**:233-243.

Oliver, JL, Q Fan, C Salvat, M Ziari, L Kong, M Mangeney and G Bereziat. **1994**. Positive and Negative Regulation of the Human Type II Phospholipase A₂ *Gene Biochemistry* **33**:7134-7145.

Oliver, S, ML Banquerigo and E Brahn **1994**. Suppression of collagen-induced arthritis using an angiogenesis inhibitor, AGM-

1470, and a microtubule stabilizer, taxol. *Cell. Immunol.* **157**:291-299.

Panda, D, JE Daijo, MA Jordan and L Wilson. **1995**. Kinetic Stabilization of Microtubule Dynamics at Steady State *in Vitro* by Substoichiometric Concentrations of Tubulin-Colchicine Complex. *Biochem.* **34**:9921-9929.

Pfeilschifter, J, H Mühl, W Pignat, F Märki and H van den Bosch. **1993**. Cytokine Regulation of Group II phospholipase A₂ expression in glomerular mesangial cells. *Eur. J. Clin. Pharm.* **44**(Suppl 1):S7-9.

Potts BC, DJ Faulkner and RS Jacobs. **1992**. Phospholipase A₂ inhibitors from marine organisms. *Journal of Natural Products.* **55**(12):1701-17.

Pruzanski, W and P Vadas. **1985**. Phospholipase A₂ activity in sera and synovial fluids in rheumatoid arthritis and osteoarthritis. Its possible role as a proinflammatory enzyme. *J. Rheum.* **12**:211-216.

Pruzanski, W and P Vadas. **1991**. Phospholipase A₂ - A Mediator Between Proximal and Distal Effectors of Inflammation. *Immunol. Today.*, **12(5)**:143-146.

Pruzanski, W, M Koo Seen Lin and P Vadas. Secretory Phospholipase A₂ in rheumataic disease, in *Clinical Inflanumtion: Molecular Approches to Pathophysiology*. K Glaser and P Vadas Eds. CRC Press, 1995. pps. 181-200.

Pruzanski, W, BP Kennedy, H van den Bosch, E Stefanski and P Vadas. **1997**. Microtubule Depolymerization Selectively Down-regulates the Synthesis of Proinflammatory Secretory Nonpancreatic Phospholipase A₂. *Lab. Invest.* **76(2)**:171-178.

Qishi, F, M Paradon, C Salavat, G Bereziat and JL Olivier. **1997**. C/EBP Factor surpression of Inhibition of Type II Secreted Phospholipase A₂ in HepG2 Cells: Possible Role for SSBP. *Mol. Cell Biol.* **17(8)**:4238-48.

Ritchlin, C, E Dwyer, R Bucala, R Winchester. **1994**. sustained and distinctive patterns of gene activation in synovial fibroblasts

and whole synovial tissue obtained from inflammatory synovitis.
Scan. J. Immun. **40(3)**:292-8.

Roshak, AK, JR Jackson, K McGough, M Chabot-Fletcher, E Mochan and LA Marshall. **1996**. Manipulation of distinct NFkappaB proteins alters interleukin-1beta-induced human rheumatoid synovial fibroblast prostaglandin E₂ formation. *J. Biol. Chem.* **271(49)**:31496-501

Roshak, A, E Mochan and L Marshall. **1996**. Supression of Human Synovial Fibroblast 85 kDa Phospholipase A₂ by Antisense reduces IL-1β-Induced PGE₂. *J. Rheum.* **23(3)**:420-427.

Roshak, A, G Sathe. and L A Marshall. **1994**. Suppression of monocyte 85-kDa phospholipase A₂ by antisense and effects on endotoxin-induced prostaglandin biosynthesis. *J. Biol. Chem.* **269**:25999-26005.

Schutze S, D Berkovic, O Tomsing, C Unger and M Kronke. **1991**. Tumor necrosis factor induces rapid production of

1'2'diacylglycerol by a phosphatidylcholine-specific phospholipase
C. Journal of Experimental Medicine, **174(5):975-88.**

Seilhamer, J, W Pruzanski, P Vadas, S Plant, J Miller, J Kloss and L
Johnson. **1989.** Cloning and Recombinant Expression of
Phospholipase A₂ Present in Rheumatoid Arthritic Synovial Fluid.
J. Biol Chem. **264(10):5335-5338.**

Shinohara, H, Y Amabe, T Komatsubara, H Tojo, M Okamoto, Y
Wakano and H Ishida. **1992.** Group II PhospholipaseA₂-induced
by Interleukin-1 β in cultures rat gingival fibroblasts. *FEBS
Letters.* **304:69-75**

Sirum-Connolly, K and CE Brinkerhoff. **1991.** Interleukin-1 or
Phorbol Induction of the stromelysin Promotor requires an
element that Cooperates with AP-1. *Nuc. Acids Res.* **19(2): 335-
341**

Solito, E And L Parente. **1989.** Modulation of phospholipase A₂
activity in human fibroblasts. *Br. J. Pharmacol.* **96:656-660.**

Suffys, P, F VanRoy. and W Fiers. **1988**. Tumor necrosis factor and Interleukin-1 activate phospholipase in rat chondrocytes

Tramposch, K, F Chilton, P Stanley, R Franson, M Havens, D Nettelton, L Davem, I Darling and R Bonney. **1994**. Inhibitor of Phospholipase A₂ Blocks eicosanoid and Platelet activating factor biosynthesis and has topical anti-inflammatory activity. *JPET*. **271**:1254-1262.

Weisman M. **1995**. Corticosteroids in the treatment of rheumatologic diseases. *Current Opinion in Rheumatology*. **7**(3):18390.

Wright, WG, CE Ooi, J Weiss and P Elsbach. **1990**. Purification of a cellular (granulocyte) and an extracellular (serum) phospholipase A₂ that participate in the destruction of *Escherichia coli* in a rabbit inflammatory exudate *J. Biol. Chem.* **265**(12):6675-668.